NIPER-196
Distribution Category UC-92

Topical Report

PREDICTIVE MODELS AND NEW SIMULATORS

Project BE2, Task 3, Milestone 1

By Raymond J. Heemstra, William D. Henline, and Mark Young

April 1987

R. M. Ray, Program Coordinator
Bartlesville Project Office
U.S. Department of Energy

Prepared for
U.S. Department of Energy
Under Cooperative Agreement DE-FC22-83FE60149

DISCLAIMER

IIT Research Institute
NATIONAL INSTITUTE FOR PETROLEUM AND ENERGY RESEARCH
P.O. Box 2128
Bartlesville, Oklahoma 74005
(918) 336-2400

TABLE OF CONTENTS

ILLUSTRATIONS

TABLES

PREDICTIVE MODELS AND NEW SIMULATORS

By Raymond J. Heemstra,* William D. Henline,** and Mark Young+

ABSTRACT

This report describes the work accomplished in FY85 and FY86 on project BE2, "Predictive Models and New Simulators," performed for the Department of Energy (DOE). The last significant reporting document on this project was Status Report NIPER-155, "Predictive Models and New Simulators," July 1986. At that time, the status of computer programming work and methodology was reported. The identification of significant EOR oil targets for light oil steamflooding and immiscible CO_2 flooding prompted work by DOE on two predictive models.

In this study, modifications were made to the DOE steamflood predictive model to include light oil behavior. Test results are shown for the new light oil steam predictive model, and comparison is made to a finite-difference simulation of a test problem. Modifications also were made to the DOE miscible flooding predictive model to include reservoir dip and another version to include immiscible flooding.

Initial test runs were provided for each of the three new predictive models. This topical report includes all work accomplished and provides a synopsis of the project from inception. Computer coding changes are described, and sensitivity analyses of computer simulations are discussed.

Tables of the changes in daily oil rates and in the cumulative oil production resulting from a 20-percent increase or decrease in the value of

* Senior Chemist.
** Project Leader.
+ Senior Engineer.

each of 35 reservoir parameters are presented. The relationships of these input variables to their results should be helpful in determining the viability of the predictive models.

A reasonable oil production history match by use of the CO_2 miscible flooding predictive model with formation dip was made and is presented. Limited predictions can be made by use of the new CO_2 immiscible predictive model.

INTRODUCTION AND BACKGROUND

In 1984, a National Petroleum Council report was published which evaluated the contribution of EOR to U.S. oil production. Five EOR process predictive models were used. Not included were light oil steamflooding and immiscible CO_2 flooding. New predictive models were deemed necessary for newly targeted oil.

This report provides a summary of all of the work performed, including that of FY85 and FY86, for project BE2. The progress generally has followed the plan recommended in the feasibility study report.[1] In that study, it was revealed that the enhanced oil recovery (EOR) processes of light oil steamflooding and immiscible CO_2 flooding have not been addressed by the various DOE EOR predictive models. Using a computer search of the National Petroleum Council (NPC) reservoir data base, performed by the DOE Bartlesville Project Office, we identified a significant EOR target for these two processes. Screening criteria used for this data search were as follows:

Light Oil Steamflooding

Oil Viscosity ≤ 100 cp

Oil saturation - porosity product ≥ 0.1 fraction

Payzone thickness ≤ 20 ft

Immiscible Gas Drive

API gravity ≈ 14°

Pressure ≥ 850 psi

Depth ≥ 1,400 ft

Based on these criteria and an assumed residual oil saturation of 35 percent after waterflood, this computer search provided the following estimates of the maximum recoverable oil for each process.

	MMSTB
Light oil steamflooding	4,602
Immiscible gas flooding	34,320

These targets were deemed sufficient to warrant addition of these processes to the suite of DOE predictive models. Actual implementation of these additions depended on technical feasibility.

The feasibility report[1] reviewed the governing equations and solution methods used in the existing DOE, heavy oil, steamflood predictive model (SFPM) and CO_2 (miscible) flood predictive model (MFPM). Changes to these methods were outlined to include the effects of light oil distillation in SFPM and a mobile immiscible gas phase in MFPM. These theoretical modifications and the required computer code changes needed to implement them in the predictive models were judged to be feasible. This report verifies this feasibility and presents model results for the two new DOE predictive models.

MODIFICATIONS TO THE DOE STEAMFLOOD PREDICTIVE MODEL TO INCLUDE LIGHT OIL BEHAVIOR

A. Scope of Work

The project results presented here are from efforts expended on computer code modifications outlined in previous reports and are initially described.[1] The latter report described a feasibility study of the current suite of DOE predictive models with regard to the need to include new models or improvements to ensure adequate predictive capabilities for all EOR processes. The criteria of significant EOR target potential and technical feasibility for modeling the technology within the usual confines of the predictive models were adhered to in deciding on new models to include. The density and distillation effects which occur in the light oil steamflood process were found to be feasible inclusions for the current DOE nonvolatile steamflood predictive model.

In FY85 and FY86 the following modifications were scheduled to update the present heavy oil predictive code.

1. Include physical, thermodynamic, and transport properties and equations to model the density and volatility effects of light oil.
2. Include relative permeability end-point determinations using capillary pressure versus saturation temperature correlations to provide estimates for residual oil after steamflooding.
3. Update the steamflood code to include steam zone gravity override effects, including simultaneous gravity and heat transfer effects.

Sections B and C describe the status of these modifications and the operable condition of the light oil steamflood predictive model.

B. Description of Equation Modification -- Previous Developments and Current Status

As a preface to this discussion, items 2 and 3 of Section A will be addressed. An examination of the DOE steamflood predictive model code has revealed a correlation first described by Williams, et al.[2] for residual oil saturation (after steamflooding) as a function of steam temperature. The equation for this correlation is shown as:

$$S_{or}^{s} = 13.253 + 2.5956 \text{ Alog } (\mu_o^s (T_s)) - 0.7196 \text{ Alog } (T_s - T_o) , \quad (1)$$

where μ_o^s = oil viscosity at steam zone temperature, CP

T_s = steam zone temperature, °F

and T_o = initial oil temperature, °F.

Residual saturations determined from capillary pressure end-points would require empirical capillary pressure curves for steam-oil and oil-brine equilibrium systems as a function of temperature. Although the use of such empirical curves would be much more accurate than neglecting them, there are almost no data for these equilibrium systems. Under these circumstances our recommendation, for now, is to retain the current correlation, equation 1.

Steam-zone, gravity-override modifications have been studied, and the fractional flow and steam zone/hot oil heat transfer effects are included within the context of the current DOE predictive code. The remainder of this section (and Section C) is devoted to a discussion of the changes incorporated to account for light oil behavior.

To account for light oil steamflooding effects, model modifications must include the capability to determine vapor/liquid equilibrium distributions between light and heavy fractions of light oil. The methodology for doing this has been discussed previously in Status Report NIPER-125, November 1985, and briefly in this report. The modifications described here involve enhancing the current steamflood model equations to account for oil vaporization. The following simplifying assumptions, consistent with the level of detail currently in the DOE predictive model, have been made:

Thermodynamic Assumptions

1. Ideal oil solutions
2. Oil insoluble in liquid water phase
3. Vapor-liquid equilibrium distributions obtained from fugacities determined from an appropriate equation of state.

Transport (Fractional Flow) Assumptions and Modifications

1. The steam zone now has significant partial pressure of hydrocarbon components, requiring modification of the fractional flow governing equations.
2. Fractional flow treatment will be modified by assuming that local thermodynamic equilibrium exists between the steam and hot liquid banks. Thus, one can write:

$$f_{s,s}\rho_{s,s} = \sum_i f_{i,s}\rho_{i,s} \qquad (2)$$

where: i = species i

Subscript (s) refers to steam zone or steam vapor,

$f_{i,j}$ = fractional flow of species i in zone j, and

$\rho_{i,j}$ = mass density of species i in zone j.

Also,

$$f_{i,s} = f(S_{i,s}, S_{j,s}; \text{---}) \tag{3}$$

where:

$S_{i,s}$ are saturations of species i in the steam zone.

These equations must be supplemented with the vapor/liquid distribution coefficients or K-values. This will close the system and allow for solution of individual species-phase saturations, $S_{i,s}$ and $S_{i,L}$, i.e. vapor (steam zone) and oil phase saturations, respectively. K-values and saturations are related as follows:

$$K_i^{(s)} = \frac{S_{i,s}}{S_{i,L}} = K_p \frac{Y_{i,s}}{X_{i,L}} \tag{4}$$

where,

K_p = a function of saturation, and

X and Y are mole species fractions in the respective phase.

Now,

$$\frac{Y_{i,s}}{X_{i,L}}, = \frac{\phi_i^L}{\phi_i^s} \tag{5}$$

where ϕ_i^j are fugacity coefficients which must be determined from an appropriate equation of state. For the steam and hydrocarbons, the Peng-Robinson correlation is a cubic equation of state which can represent this system. Therefore,

$$\ln\phi_i = (RT)^{-1} \int_o^p \left[\left(\frac{\partial V}{\partial n_i}\right)_{T,p,n_j} - \frac{RT}{p'}\right] dp' \qquad (6)$$

and

$$P = \frac{RT}{V-b} - \frac{a(T)}{V(V+b) + b(V-b)} \cdot \qquad (7)$$

Parameters a(T) and b, which appear in equation 7, must be determined from data specific to the water (steam)-hydrocarbon system of interest. This amounts to empirically determining system species binary interaction coefficients.

In the latter part of FY85 and the early part of FY86, software routines were written to implement a Peng-Robinson equation-of-state (EOS) based isothermal flash calculation for an example steam-light oil system. Binary interaction parameters and critical constants were estimated using known constants, empirical molecular weights, and normal boiling temperatures for representative oil fractions (distillation cuts) for a sample oil.[3] Table 1, also taken from reference 2, lists properties of six hypothetical component fractions which have been used to test the Peng-Robinson EOS based equilibrium flash routines.

TABLE 1. - Empirical properties of typical crude oil (23° API)

Component	Mol Wt	Boiling Point, ° F	Density, g/cm^3	Mol Frac
1	145.50	372.83	0.8253	0.1860
2	208.91	536.93	0.8776	0.2862
3	288.54	698.77	0.9131	0.2223
4	390.44	874.75	0.9410	0.1505
5	495.74	1042.70	0.9611	0.0869
6	609.13	1218.08	0.9775	0.0681

Average molecular weight = 294.3
Average density = 0.9165 (22.9° API)

Trial calculations were attempted for systems of seven components (i.e. oil + water) at various temperatures (400° to 600° F), pressures (150 to 600 psig), and initial steam-to-oil ratios of (5:1 to 30:1). This set of computer subroutines was initially tested for a widely known and essentially ideal light hydrocarbon system (e.g., methane, ethane, propane and butane). Flash calculations converged rapidly; however, in the steam/oil system, convergence was so slow it would be considered impractical to reach a solution. This was true for all conditions of temperature, pressure, and composition. The strong non-ideal nature of water-oil component solution interactions requires detailed empirical data for adequate EOS prediction. Given such data, the use of EOS-based flash calculations will require excellent initial estimates to reach rapid solution convergence. Having concluded this, we chose an alternate scheme to determine individual component K-values. The functional expression, for component i,

$$K_i = (P_{r_i})^{-1} \exp[5.37\ \omega_i(1 - 1/T_{r_i})], \tag{8}$$

$$\omega_i = 3/7\ [(T_{B_i}/T_{c_i})/(1 - T_{B_i}/T_{c_i})]\ \log_{10}(P_{c_i}/P_A) \tag{9}$$

$T_{r_i} = T/T_{c_i}$ T_{B_i} = normal boiling temperature, °F (10)

$P_{r_i} = P/P_{c_i}$ T_{c_i}, P_{c_i} = critical values (11)

P_A = atmospheric pressure, psi

presented by Wilson[4] is now used to determine system bubble points, dew points, and vapor/liquid isothermal flash partitions. For hydrocarbon systems, this correlation is expected to be acceptable for pressures to 500 psia.

Separate subroutines, based on equation 8, were written to evaluate bubble points, dew points, and flash partitions. Each routine requires input values for temperature, pressure and total system composition. In this configuration, vapor/liquid ratios and resultant phase compositions can be directly used in the INTCMP subroutine heat and material balance calculations or (in principle) used as initial estimates for an EOS-based flash calculation. At this point, the subroutines that use EOS procedures have not been merged with the light oil steamflood model. Since few thermodynamic data are available, such subroutines should not be included until the empirical K-value correlation (equation 8) is tested further for actual light oil steamfloods.

The thermodynamic, flash routines based on K-values (equation 8) have been tested over a range of temperatures and pressures typical of steamflooding conditions (400° to 500° F and 400 psia). Initial tests were run with six oil components plus water comprising the complete thermodynamic system. In most cases, unreasonable values ranging in excess of 1,200° F were obtained for system bubblepoints, even with high initial concentrations of water.

Figure 1 shows a plot of the temperature dependence (ln K vs 1/T) of the test system for component critical and normal boiling point properties derived from properties given in table 2. As shown in figure 1, components 1 and 2 represent the volatile segment of the system. Steam at very high temperatures (> 700° F) becomes a volatile component when considered as part of the total system and when equation 8 is used as the K-value for steam. In the range of steamflooding (~ 400° to 500° F), water is nonvolatile relative to the system light end components 1 and 2. This behavior demonstrates the inability for the K-value correlation to predict the steam/hydrocarbon solution nonidealities. To counter this difficulty, an additional thermodynamic assumption has been added to the previous list. It is now being assumed that in addition to oil being insoluble in the water phase, water is essentially insoluble in the oil phase. The nonideality of the steam-hydrocarbon system would suggest that this is a reasonable assumption. Under these assumptions, the K-value based flash subroutines give reasonable limits for dew points and bubble points. In this mode, water behaves as a diluent in the flash calculations.

Meshing of the K-value routines with the fractional flow and energy balance calculations in the light oil steamflood computer program has been accomplished, and several test runs have been made. These runs will be discussed in detail in Section D. Some reference to these results is made here to clarify the current status of modifications to the fractional flow calculations for the light oil system. At present, the fractional flow equations assume that all gas and liquid phase species have the same relative permeability as the combined phase; that is, no compositional effect has been included, as per equation 2, in fractional flow calculations.

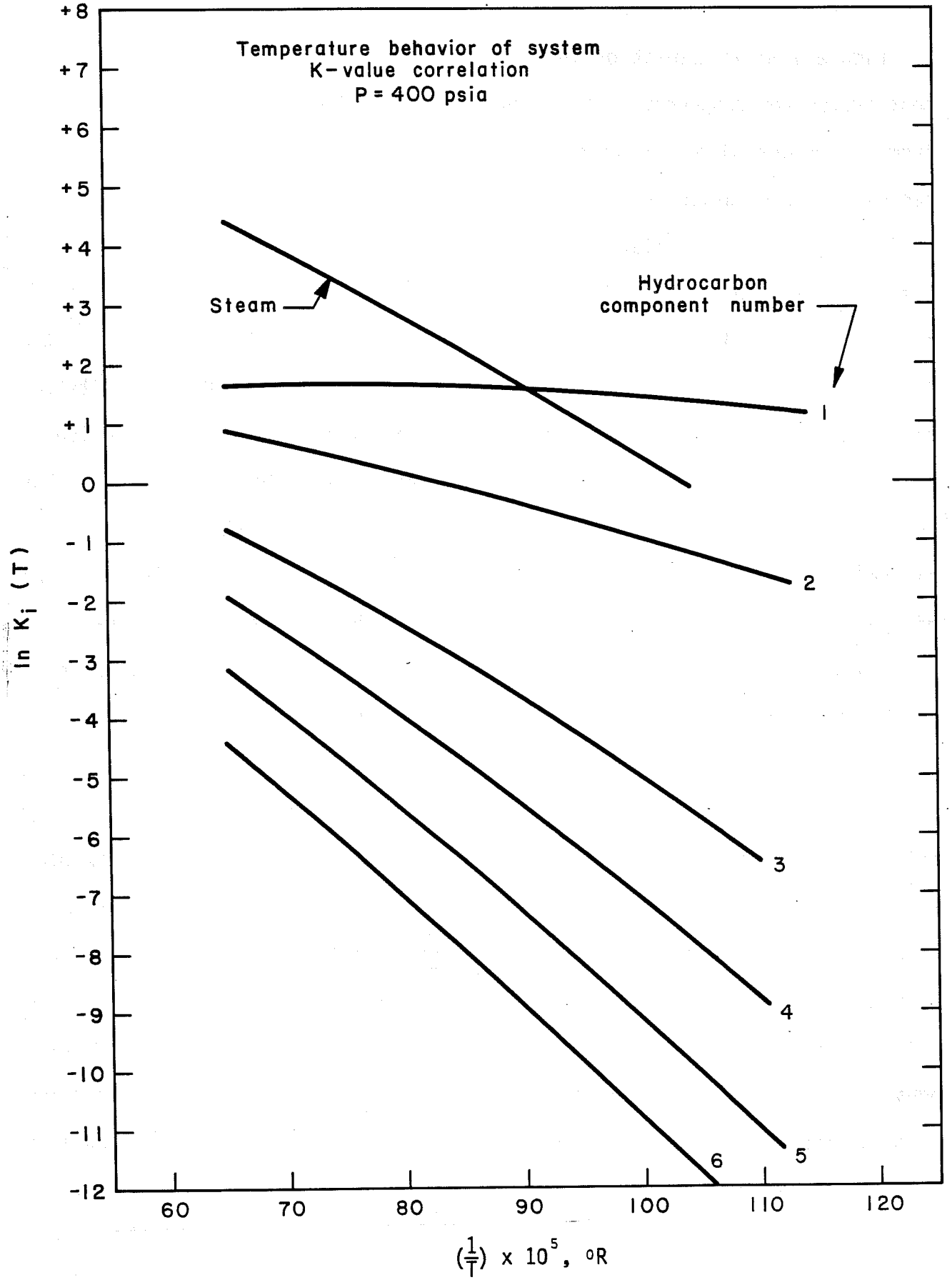

FIGURE 1. - Temperature dependence of system component K-value correlation.

TABLE 2. - Input requirements for LOSFPM representing the equivalent SPE light oil steamflood test problem

Formation depth, ft subsea	1500
Initial pressure, psig	75
Initial temperature, °F	125
Formation gross thickness, ft	80
Formation net pay, ft	80
Formation average permeability, md	1100
Formation average porosity, fraction	0.30
Rock density at steam temperature, lb/ft^3	165.0
Rock heat capacity, BTU/lb °F	0.20
Rock diffusivity, ft^2/hr	0.0306
Total pattern area, acres	2.5
Initial oil saturation, PV	0.55
Initial gas saturation, PV	0.0
Initial water saturation, PV	0.45
Oil gravity, °API	22
Oil viscosity, cp	265
Well radius, ft	0.3
Sandface steam quality, @ 450°F	0.7
Steam injection rate, bbl/d CWE	300

Initial Oil Properties

	Component		
	1	2	3
Mole fraction	0.5030	0.1614	0.3356
Mol. wt.	250	450	600
P_c, psia	225	140	---
T_c, °F	800	950	---
Heat capacity, BTU/lb	0.53	0.55	0.66
Density, lb/ft^3	52.3	57.64	61.2
Viscosity, cp	1.77	8	784

Changes in phase saturation (i.e. S_g [steam phase], S_L [water phase] and S_o [oil phase]) are determined from heat and material balances as before, but are now further updated by the flash calculations. Density, viscosity, formation volume factors, etc. for each phase are determined as before in the original steamflood predictive model. Phase, physical and thermodynamic properties are functions of species composition in the equilibrium flash calculations.

A quantitative estimate of the magnitude of the effect of these assumptions can be obtained only by efforts beyond the scope of this study. This would involve updating all existing subroutines that process input data as well as expanding input data requirements. These updates would also necessitate building in prescribed default values for individual component densities, viscosities, molecular weights, boiling points, etc.

It is recommended that an effort of this magnitude be delayed indefinitely until the light oil steamflood model can be compared, in its present form, with a definitive finite-difference, thermal simulator. Results of parameter studies (Section D), which varied API gravity and oil composition (in terms of vaporization), show that these effects may be dominant. Changes in flow properties and heat effects, due to composition, are unlikely to cause variations in the above parameters as large as the variations shown in these results.

C. Computer Code Changes and Flowsheet of Modifications

This section will describe the methods used to implement the modifications alluded to in Section B to update the original DOE steamflood predictive model to describe both light and heavy oil behavior. A description of changes made

to each impacted subroutine will be given, and the relation to other code elements will be provided. An overall logic diagram of the new (light oil) code is shown in figure 2.

Currently, the light oil steamflood predictive code is called LOSFPM and has been developed by modifying the DOE predictive code SFPM (steamflood predictive model). Specific computer program modifications begin with updating subroutine IPUT to include input values of composition, critical properties, normal boiling points, etc. for oil components. The following data are read directly into IPUT by the user.

YQ(I = 1,7), initial vapor species mole fraction;
I = 7 is for water

XQ(I = 1,7), initial liquid phase species mole fraction
I = 1,6 for oil, I = 7 for water

DENB(I = 1,6), oil pseudo-component
density, [LB/FT^3]

BMW(I = 1,6), oil component molecular weights.

Subroutine IPUT calls an additional routine named RECALT which supplies data for component normal boiling points (TBA(I)), critical temperatures (TCB(I)), and critical pressures (PC(I)). RECALT also uses these values to calculate component accentric factors used in component K-value equations. All other input variables and subroutines in LOSFPM are the same as those for SFPM.

Remaining changes to SFPM have occurred entirely within the primary subroutine INTCMP. This large body of code uses the expanding tank steamflood model equations previously documented.[5] As mentioned in Section B, these equations have been updated to redistribute volatile oil components between the liquid, oil, and vapor (primarily steam) phases. By use of simultaneous

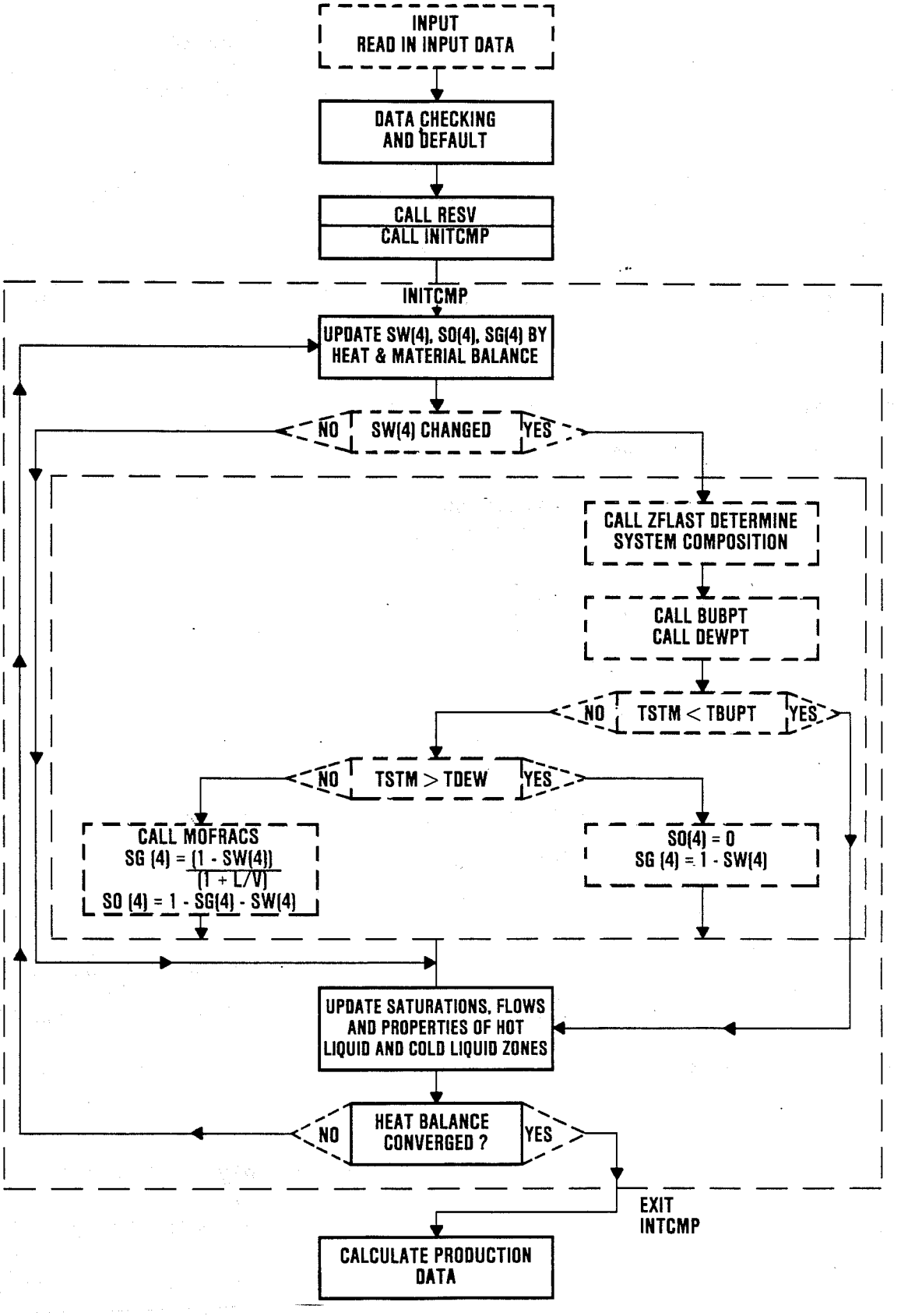

FIGURE 2. - Logic diagram for modifications embodied in LOSFPM. Dotted boxes refer to routines changed or added to original program SFPM. (SW(4), SO(4), and SG(4) are aqueous, oleic, and vapor phases in the steam zone.)

energy balances and fractional flow, the algorithm that comprises INTCMP is designed to update steam-zone (vapor) (SG(4)), liquid (water) (SW(4)) and liquid oil (SO(4)) saturations in the steam zone for each incremental time step. Within each time step, for a fixed steam temperature, saturations are iteratively determined from a steam-zone heat loss, successive relaxation procedure. For a given time step, when enthalpy injected is balanced with reservoir losses, a solution for determining saturations is achieved.

To modify this scheme to account for light oil vaporization, each time new trial values for steam-zone saturations are obtained by heat and material balance, an isothermal flash calculation must be made to readjust these saturations to be consistent with the phase distribution equilibrium in the vapor and liquid states. Since the liquid water phase is not involved in the flash determination, phase redistributions are performed with SW(4) held constant. Under this scenario, a change in SW(4) during update will result in a recalculation of SG(4) and SO(4), (SO(4) + SG(4) + SW(4) = 1) with SO(4) always being considered equal to the steam-zone residual oil saturation; that is, oil is not considered to be mobile in the steam zone.

These "new" trial values of SG(4) and SO(4) are used to determine new values for the total system species (oil components + water) composition for the system (oil phase + vapor phase) and to provide initial estimates for phase partition (L/V) for subsequent flash calculations. Given this information, current values for system bubblepoints and dewpoints are calculated from subroutines BUBPT and DEWPT, respectively. If the steam zone temperature is below the bubblepoint, no flash calculation is performed. If the temperature is above the dewpoint, then all oil is vaporized; i.e. SO(4)→SOR(4) where SOR(4) is the residual oil saturation in the steam zone. For temperatures within the bubblepoint-dewpoint range, an isothermal flash is performed by

subroutine MOFRACS. The resultant updated ratio of liquid (oil)-to-vapor is used to further update the values of SG(4) and SO(4) such that SW(4) remains unaffected. The sequence of programming steps in INTCMP, which accomplishes this, is shown in appendix A in FORTRAN code. This segment occurs immediately after heat and material balance update of SW(4). Subroutine ZFLAST calls BUBPT, DEWPT and MOFRACS for the bubblepoint, dewpoint and equilibrium flash calculations, respectively. FORTRAN source listings of these subroutines are given in appendix B. Subroutine ZBLAST is an abbreviated version of ZFLAST designed to provide system compositional updates.

Updated values for oil saturation, after the flash calculation, are checked against the residual value, SOR(4). If SO(4) is less than the current SOR(4), SOR(4) is set equal to SO(4). In this manner, residual oil saturations after steamflooding can, in principle, be reduced to zero.

Figure 2 displays the overall logic flow of the events narrated above.

D. Discussion of Light Oil Test Cases and Comparison to Heavy Oil Steamflooding

Light oil systems subject to steamflooding will have at least two primary characteristics which differ greatly from those of heavy oil thermal recovery: (1) higher API gravity (greater than 25°), and (2) higher volatility due to higher concentrations of low-boiling hydrocarbon fractions. These property differences usually occur simultaneously, and to test the predictive behavior of this new light oil steamflood model properly, the effects of changes in API gravity and volatility have been investigated separately, providing both a qualitative and quantitative measure of each effect.

Sensitivity studies of the effects of API gravity and volatility were performed for the oil composition cases shown in table 3.

Table 3. - Selected oil composition cases.

API Gravity, degrees

Volatility	15° Non-volatile	35° Non-volatile	45° Non-volatile
	-	α_1	β_1
	-	α_2	β_2
	-	α_3	-
	-	α_4	-

where α_i and β_i represent different crude oil compositions as follows:

Crude oil compositions, mole fraction

Component[1]	Non-volatile	α_1	α_2	α_3	β_1	α_4, β_2
1	0	0.75	0.25	0.05	0.75	0.04
2	0	0.25	0.65	0.65	0.25	0.14
3	0	0	0.10	0.30	0	0.63
4	0.60	0	0	0	0	0.19
5	0.30	0	0	0	0	0
6	0.10	0	0	0	0	0

[1] In order of decreasing volatility.

Using LOSFPM, we performed simulations for each of these cases, and results are presented in figures 3 through 7 as cumulative production of oil and gas. This form of presentation was chosen since these curves contain information about rates and total production (recovery). Figure 3 shows the effect of solely varying API gravity for a non-volatile oil. The effect of high initial viscosity on oil fractional flow is evident in the 15° API case. Also, the primary difference among these cases is in the initial timing. Total recoveries are essentially the same. Differences in timing can, of course, affect project economics.

Cumulative gas production, a function of API gravity, shows similar results in figure 4 but more total gas production for lighter oils. This would be a result of more gravity override due to lower density and higher gas mobility at lower viscosities. Figures 5 and 6 show the effect of increasing volatility for 35° and 45° API oils. The trend is toward higher rates and recovery for more volatile oils. The recoveries are near 100 percent of OOIP. Also, figure 7 indicates higher gas rates for volatile oils.

E. Test Comparison of the Light Oil Steam Predictive Model and a Finite-Difference Test Problem

As a calibration check, it would be desirable to compare the predictive model with an actual steam distillation, field pilot test. Data of this nature are rare. Instead, a comparison has been run against a test problem designed to evaluate state-of-the-art, finite-difference, thermal-compositional simulators. Results of a light oil steam simulation performed by Chevron, Computer Modeling Group, and Scientific Software-Intercomp have been calculated, and Aziz and Ramesh[6] have discussed these individual calculations in detail. These results were determined for a single 5-spot production well and were based on the reservoir and operating conditions listed in table 2.

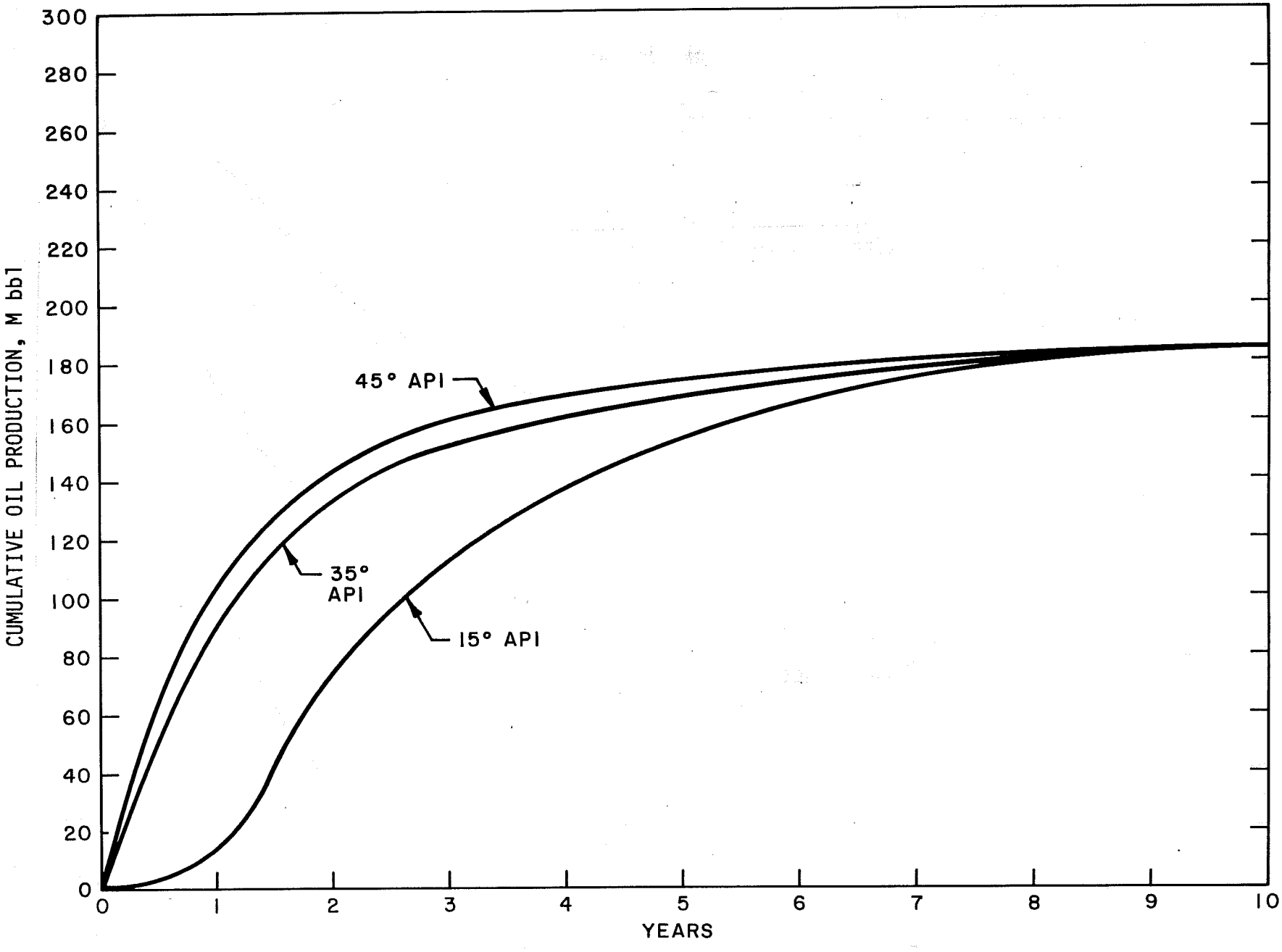

FIGURE 3. - Effect of API gravity on oil production timing.

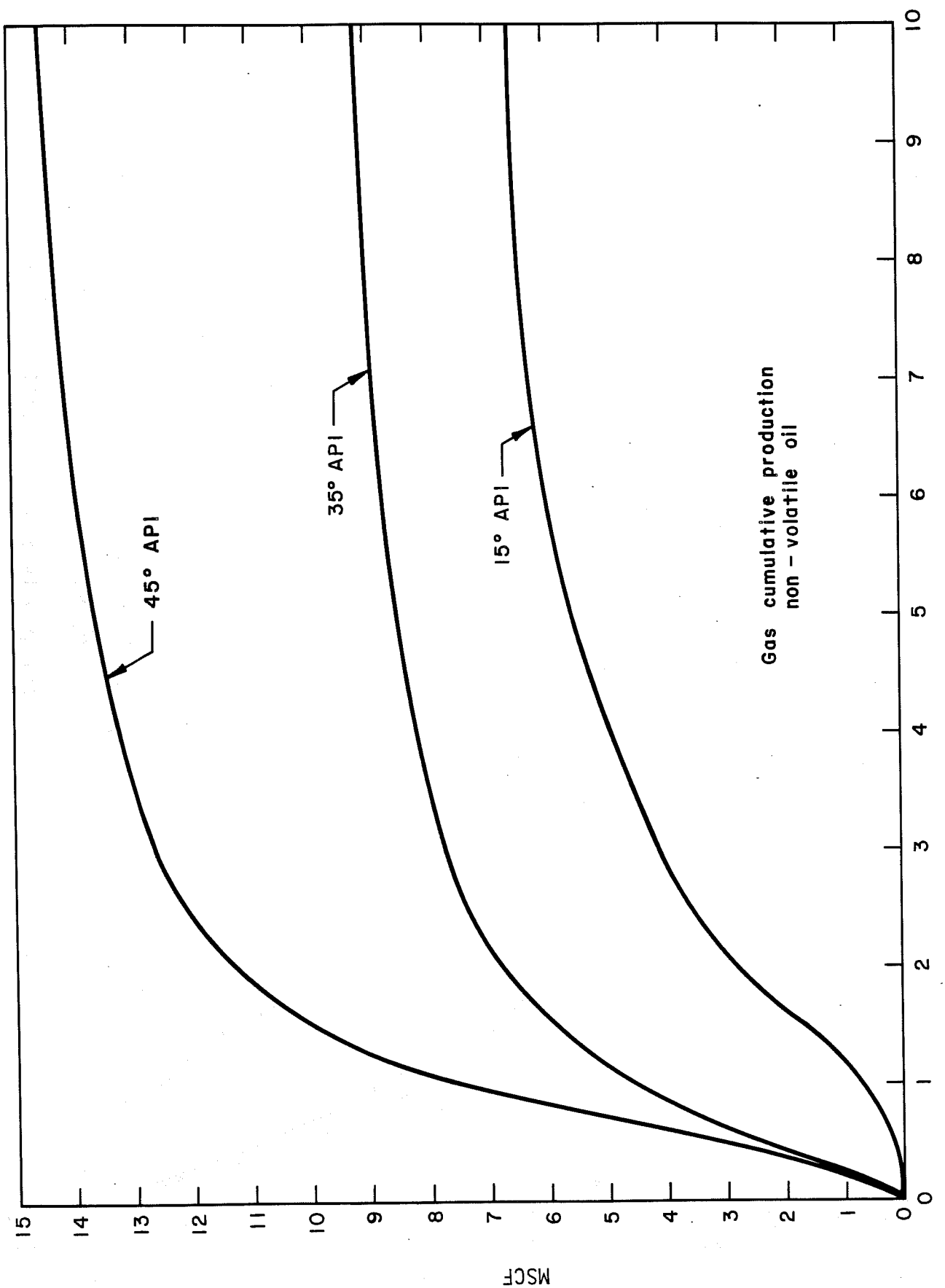

FIGURE 4. - API gravity effect on gas production and recovery.

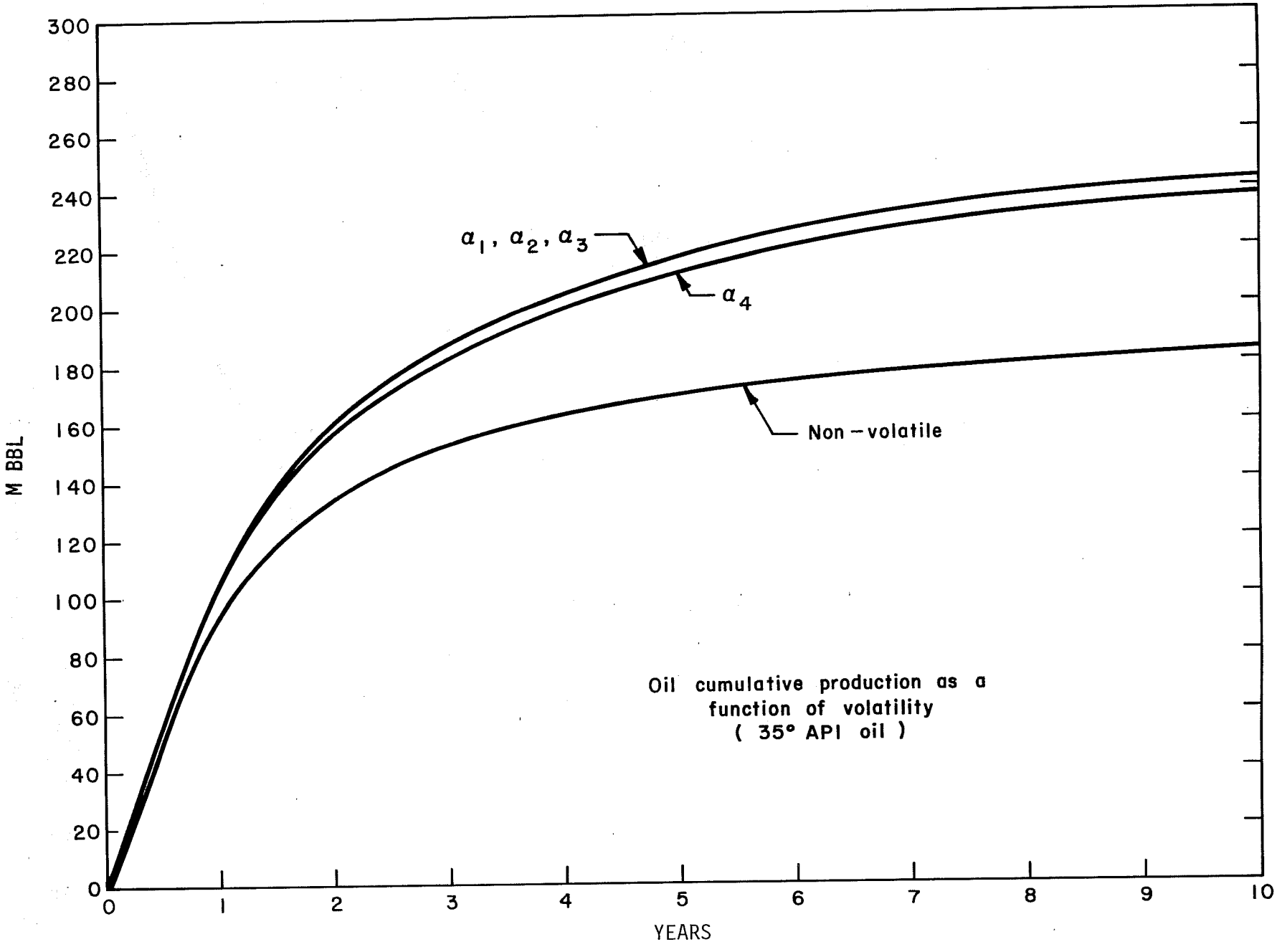

FIGURE 5. - Oil production dependence on volatility (35^{o} API oil).

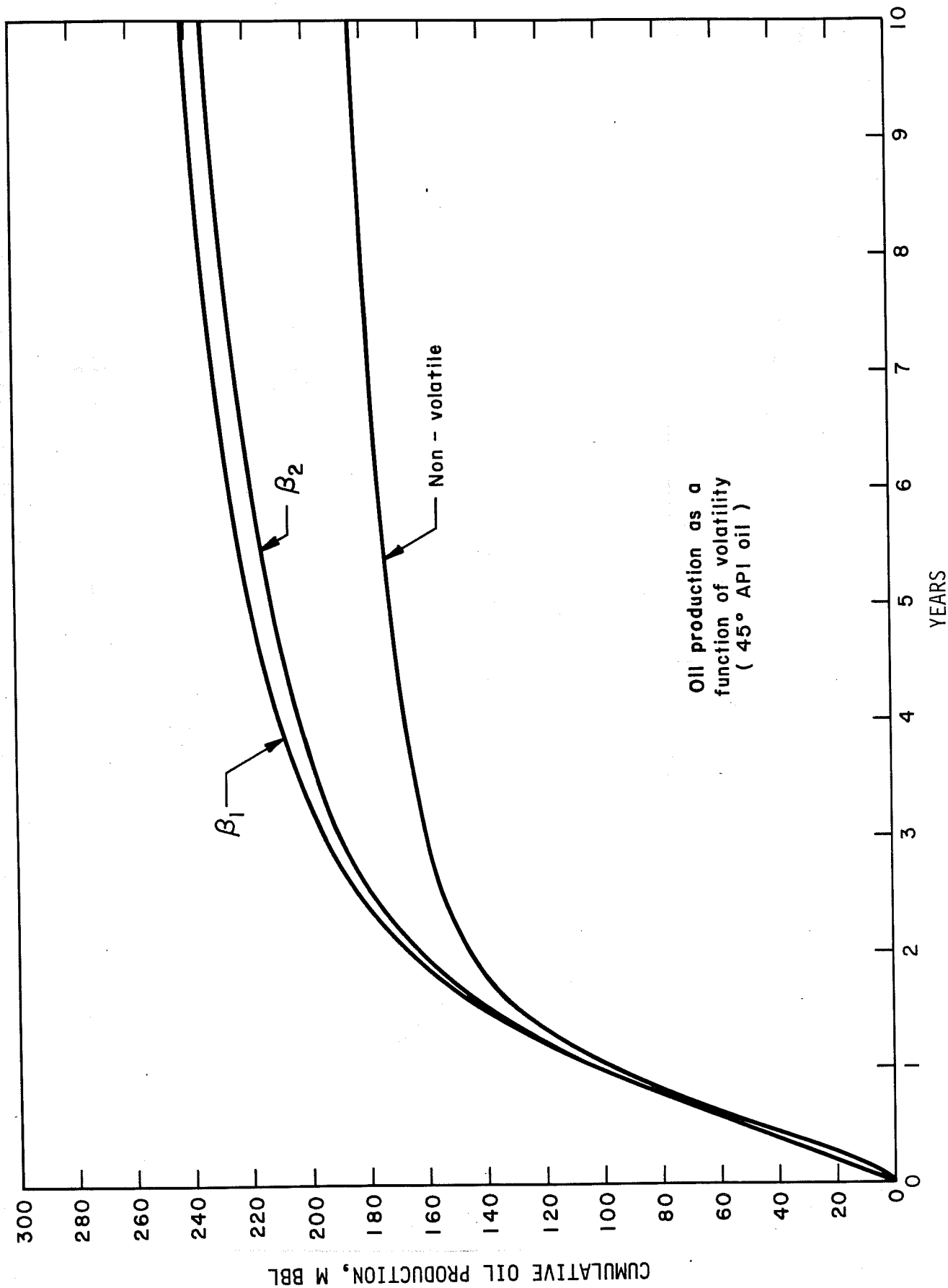

FIGURE 6. - Oil production dependence on volatility (45^0 API oil).

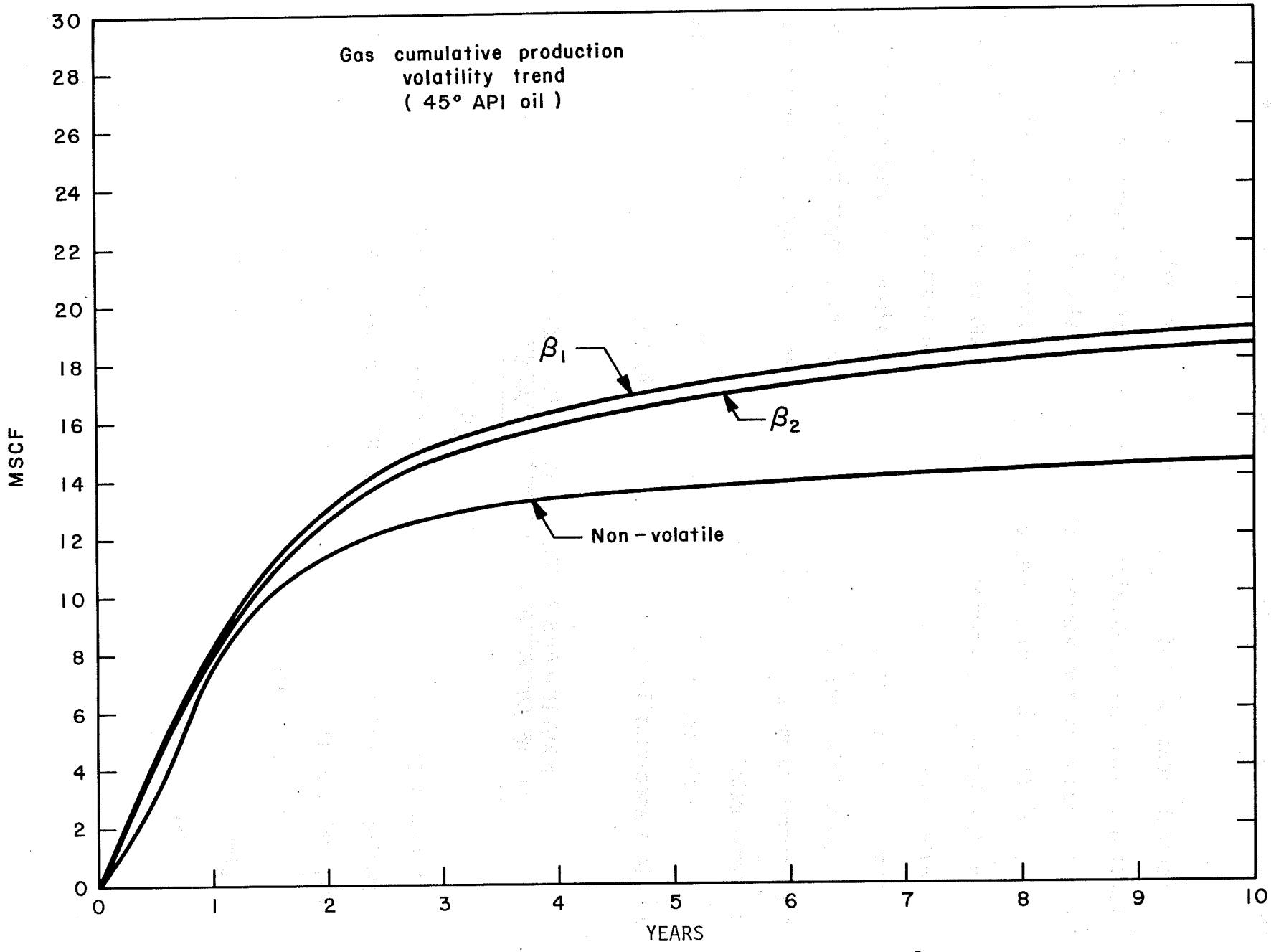

FIGURE 7. - Gas production depencence on volatility (45^{o} API oil).

These values are listed in the required format and represent entries needed in LOSFPM.

Several runs of LOSFPM were made with these data and the existing vapor/liquid equilibrium K-values. The results fall in a narrow band around those predicted by the various finite-difference simulators. This band of results is obtained from LOSFPM by varying the initial oil composition and keeping the API gravity constant. Figure 8 shows the various results in terms of cumulative oil production for a single, inverted 5-spot production well.

Figure 8 reveals that the predictive model can adequately predict recovery and project life, but that initial rates are not very representative. The more comprehensive simulators predict a breakthrough of light-end components at approximately 2½ years. This will not occur with the predictive model since no mechanism in the calculational algorithm has been provided to calculate specifically the recovery of a light hydrocarbon bank.

MODIFICATIONS TO THE DOE CO_2 (MISCIBLE) PREDICTIVE CODE TO INCLUDE RESERVOIR DIP AND IMMISCIBLE GAS FLOODING

A. Scope of Work

In fiscal year 1985, NIPER conducted a study to determine the feasibility of developing predictive models not in DOE's system. As a result of this study, the DOE CO_2 (miscible) flood predictive code was chosen for modification to include immiscible flooding and to account for reservoir dip. This selection was predicated on the fact that a significant EOR potential existed where these modified models could be applied.

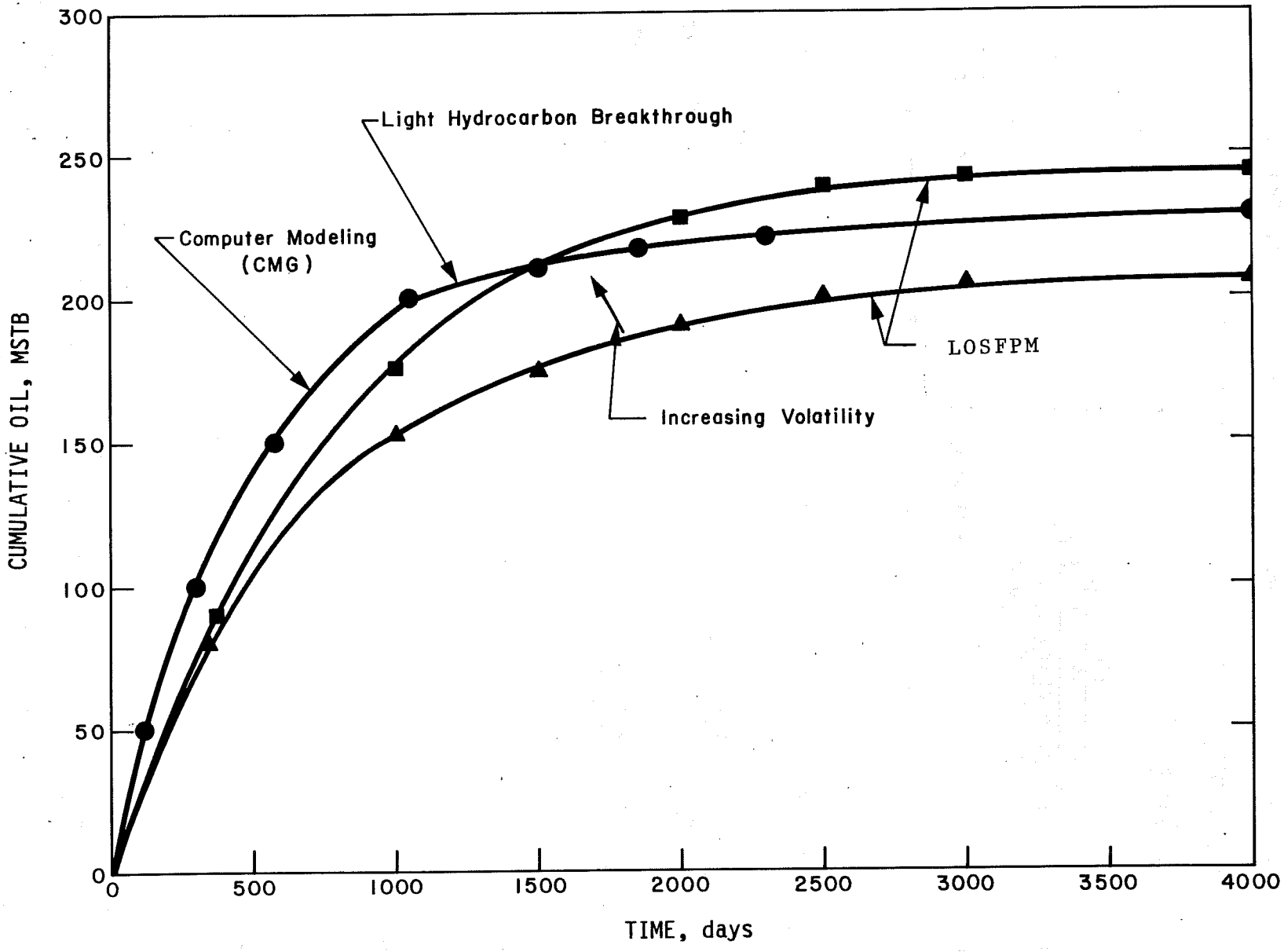

FIGURE 8. - Comparison of cumulative production predicted by a finite-difference simulator with that of two LOSFPM runs with varying crude oil volatility.

B. Equation Development for Reservoir Dip

After a review of DOE documentation,[7] an analysis of the fractional flow equations used in MFPM led to the following revised equations to include dip, as previously reported.[1]

$$f_j = \frac{(1 + \frac{g\sin\alpha}{\nabla P}\rho_j)\lambda_j}{\sum_j \lambda_j + \frac{g\sin\alpha}{\nabla P}\sum_j \rho_j \lambda_j} \quad (j = 1,2,3)$$

A re-examination of these equations indicated that they are inappropriate and a new set of fractional flow equations was developed from first principles as follows:

From Darcy's law:

$$q_w = -\frac{K_w A}{\mu_w}\left[\frac{\partial P}{\partial X}w + \rho_w g\sin\alpha\right] \tag{12}$$

$$q_o = -\frac{K_o A}{\mu_o}\left[\frac{\partial P}{\partial X}o + \rho_o g\sin\alpha\right] \tag{13}$$

$$q_g = -\frac{K_g A}{\mu_g}\left[\frac{\partial P_g}{\partial X} + \rho_g g\sin\alpha\right] \tag{14}$$

The capillary pressures are defined as:

$$P_{cwo} = P_o - P_w \tag{15}$$

$$P_{cog} = P_o - P_g \tag{16}$$

$$P_{cwg} = P_w - P_g \tag{17}$$

substituting equation 15 into 13:

$$q_o = - \frac{K_o A}{\mu_o} \left[\frac{\partial P}{\partial X} c_{wo} + \frac{\partial P}{\partial X} w + \rho_o g \sin\alpha \right] \tag{18}$$

solving for $\frac{\partial P}{\partial X} w$ in equation 12 and substituting into 18:

$$q_o = - \frac{KA}{\mu_o} \left[- \frac{\mu_w q_w}{K_w A} + \frac{\partial P}{\partial X} c_{wo} - \Delta\rho_{wo} g \sin\alpha \right] \tag{19}$$

where $\Delta\rho_{wo} = \rho_w - \rho_o$

Now by definition:

$$q_w = f_w q \tag{20}$$

where f_w = fractional flow of water

$$q = q_w + q_o + q_g \tag{21}$$

and $$q_o = (1 - f_w - f_g) q = f_o q \tag{22}$$

substituting equations 20 and 22 into 19:

$$(1 - f_w - f_g) q = - \frac{K_o A}{\mu_o} \left[- \frac{\mu_w f_w q}{K_w A} + \frac{\partial P}{\partial X} c_{wo} - \Delta\rho_{wo} g \sin\alpha \right] \tag{23}$$

We now require f_g to solve for f_w.

Substituting equation 17 into 14:

$$q_g = - \frac{K_g A}{\mu_g} \left[- \frac{\partial P_{cwg}}{\partial X} + \frac{\partial P_w}{\partial X} + \rho_g g \sin\alpha \right] \tag{24}$$

substituting $\frac{\partial P_w}{\partial X}$ from equation 12 into 24:

$$q_g = - \frac{K_g A}{\mu_g} \left[- \frac{\mu_w q_w}{K_w A} - \frac{\partial P_{cwg}}{\partial X} - \Delta\rho_{wg} g \sin\alpha \right] \tag{25}$$

where $\Delta\rho_{wg} = \rho_w - \rho_g$

substituting $q_g = f_g q$ and $q_w = f_w q$ into (25)

and solving for f_g:

$$f_g = - \frac{K_g A}{\mu_g q} \left[- \frac{\mu_w f_w q}{K_w A} - \frac{\partial P_{cwg}}{\partial X} - \Delta\rho_{wg} g \sin\alpha \right] \tag{26}$$

substituting equation 26 into 23 and solving for f_w yields:

$$f_w = \frac{1 + \frac{K_o A}{\mu_o q} \left[\frac{\partial P_{cwo}}{\partial X} - \Delta\rho_{wo} g \sin\alpha \right] - \frac{K_g A}{\mu_g q} \left[\frac{\partial P_{cwg}}{\partial X} + \Delta\rho_{wg} g \sin\alpha \right]}{1 + \frac{\mu_w}{\mu_o} \frac{K_o}{K_w} + \frac{\mu_w}{\mu_g} \frac{K_g}{K_w}} \tag{27}$$

A similar set of substitutions yields an expression for f_o:

$$f_o = \frac{1 - \frac{K_g A}{\mu_g q} \left[\frac{\partial P_{cog}}{\partial X} + \Delta\rho_{og} g \sin\alpha \right] - \frac{K_w A}{\mu_w q} \left[\frac{\partial P_{cwo}}{\partial X} - \Delta\rho_{wo} g \sin\alpha \right]}{1 + \frac{\mu_o}{\mu_w} \frac{K_w}{K_o} + \frac{\mu_o}{\mu_g} \frac{K_g}{K_o}} \tag{28}$$

and

$$f_g = 1 - f_w - f_o \tag{29}$$

In the CO_2 predictive codes, capillary pressure is neglected, and "mixture" viscosities (μ') are used for water and oil. The fractional flow equations then take the final form:

$$f_w = \frac{(1\text{-}0.49828X10^{-6}\ \frac{K_o A}{\mu_o' q}\ \Delta\rho_{wo} g\sin\alpha - 0.49828X10^{-6}\ \frac{K_g A}{\mu_g q}\ \Delta\rho_{wg} g\sin\alpha)}{1 + \frac{\mu_w' K_o}{\mu_o' K_w} + \frac{\mu_w'}{\mu_g}\frac{K_g}{K_w}} \tag{30}$$

$$f_o = \frac{(1\text{-}0.49828X10^{-6}\ \frac{K_g A}{\mu_g q}\ \Delta\rho_{og} g\sin\alpha + 0.49828X10^{-6}\ \frac{K_w A}{\mu_w' q}\ \Delta\rho_{wo} g\sin\alpha)}{1 + \frac{\mu_o'}{\mu_w'}\frac{K_w}{K_o} + \frac{\mu_o'}{\mu_g}\frac{K_g}{K_o}} \tag{31}$$

and as before $f_g = 1 - f_w - f_o$

Since the fractional flows are based on a one-dimensional displacement (slim tube model),[8] no mixing between the oleic phase and the aqueous phase is assumed with each phase held at equilibrium viscosity and having well mixed components.

The factor $0.49828X10^{-6}$ provides for consistent units.

$$A = ((43560)\text{AREA})^{\frac{1}{2}}\ \text{THICK}$$

where AREA = Area of reservoir under CO_2 flood

THICK = Reservoir thickness.

μ_o' and μ_w' are "mixture" viscosities given by:

$$\mu_w' = \left[\frac{1}{\frac{C(1,1)}{\mu_w^{1/4}} + \frac{C(2,1)}{\mu_o^{1/4}} + \frac{C(3,1)}{\mu_g^{1/4}}}\right]^4 \tag{32}$$

$$\mu_o' = \left[\frac{1}{\frac{C(1,2)}{\mu_w^{1/4}} + \frac{C(2,2)}{\mu_o^{1/4}} + \frac{C(3,2)}{\mu_g^{1/4}}}\right]^4 \tag{33}$$

where μ_w = pure water viscosity

μ_o = pure oil viscosity

μ_g = pure CO^2 viscosity

$C(i,j)$ = volume fraction of species i in phase j $\begin{cases} i = 1,2,3 \\ j = 1,2,3 \\ \text{(water, oil, } CO_2\text{)} \end{cases}$

K_o, K_w, K_g = oil, water and gas effective permeabilities

The effective permeability for a given phase is the product of absolute permeability and relative permeability. The relative permeabilities were reformulated in IFPM to account for three phases. Explicit expressions for these relative permeabilities are:

$$KR1 = KR1E \left[\frac{S(1) - S1R}{1-S1R-S2R-S3R}\right]^M \tag{34}$$

$$KR2 = KR2E \left[\frac{S(2)-S2R}{1-S1R-S2R-S3R}\right]^N \tag{35}$$

$$KR3 = KR3E \left[\frac{S(3)-S3R}{1-S1R-S2R-S3R}\right]^{MN} \qquad (36)$$

where KR1E, KR2E, KR3E = water, oil, gas end-point relative permeabilities

S(1), S(2), S(3) = water, oil, gas saturations

S1R, S2R, S3R = water, oil, gas residual saturations

M, N, MN = experimentally determined exponents

C. Theoretical Modifications Required to Include Immiscible Gas

The CO_2 miscible flood predictive model (MFPM) is based on the solution of a set of partial differential equations describing mass conservation in one dimension. These equations are given by:

$$\frac{\partial C_i}{\partial t_D} + \frac{\partial F_i}{\partial X_D} = 0 \qquad (37)$$

where $i = 1 \equiv$ water
$i = 2 \equiv$ oil
$i = 3 \equiv CO_2$

X_D = dimensionless distance = X/L

t_D = dimensionless time in pore volumes = $\int_o^t q dt/V_p$

C_i = overall concentration of species i

$$C_i = C_{i1}S_1 + C_{i2}S_2 \quad , \; i = 1,2,3 \tag{38}$$

C_{ij} = concentration of species i in phase j

$$F_j = C_{i1}f_1 + C_{i2}f_2, \; i = 1,2,3 \tag{39}$$

where f_j and S_j are the fractional flow and saturation of phase j.

In MFPM the oil contribution to the fractional flux is modified to take into account the effect of viscous fingering. This is done by adopting the theory originally proposed by Koval.[9] With this modification, the equations for overall fractional fluxes become:

$$F_i = C_{i1}f_1 + f_{i2}f_2 \tag{40}$$

where

$$f_{32} = \frac{C_{32}}{C_{12}\left(\frac{\mu_3{}^0}{\mu_1{}^0}\right) + \frac{C_{22}}{K_{val}} + C_{32}} \tag{41}$$

$$f_{22} = \frac{C_{22}/K_{val}}{C_{12}\left(\frac{\mu_3{}^0}{\mu_1{}^0}\right) + \frac{C_{22}}{K_{val}} + C_{32}} \tag{42}$$

$$f_{12} = 1 - f_{22} - f_{32} \tag{43}$$

and $\mu_1{}^0$ = pure water viscosity

$\mu_3{}^0$ = pure CO_2 viscosity

$$K_{val} = \text{Koval factor} = H[0.78+0.22(\mu_2^0/\mu_3^0)^{1/4}]^4 \quad (44)$$

where μ_2^0 = pure oil viscosity

H = heterogeneity factor defined by

$$\log_{10}H = VDP/(1-VDP)^{0.2} \quad (45)$$

where VDP = Dykstra-Parsons coefficient

In MFPM, CO_2 is assumed to be completely miscible in both an aqueous phase and an oleic (oil) phase. Therefore, at each point on a locus of compositions $C_i(X,t)$ through the reservoir (in this case, 1-dimensional), local thermodynamic phase equilibrium is guaranteed between aqueous and oleic phases by the summation,

$$\sum_{i=1}^{3} C_{i2} - \sum_{i=1}^{3} C_{i1} = \sum_{i=1}^{3} \frac{C_i(K_j - 1)}{1+S_2(K_i-1)} = 0 \quad (46)$$

and

$$C_{i1} = \frac{C_i}{1+S_2(K_i-1)} \quad (47)$$

with

$$C_{i2} = C_{i1}\, K_i \quad (48)$$

To include a third (immiscible) gas phase, with saturation S_3 equations 38 and 40 must be modified. To prevent having to perform a complete three-phase equilibrium flash calculation, as a first approximation, the physical problem will be presumed to behave as if essentially no oil or water vaporized into the gas phase. This is not an unreasonable assumption at high pressures and moderate temperatures, especially in heavy oil systems. The alternative of solving the complete three-phase system would require a complex algorithm,

and is beyond the scope of this work. With these assumptions regarding non-volatility, equations 38 and 40 become

$$\begin{aligned} C_i &= C_{i1}S_1 + C_{i2}S_2 + S_3 \\ F_i &= C_{i1}f_1 + f_{i2}f_2 + f_3 \end{aligned} \qquad i = 3 \tag{49}$$

$$\begin{aligned} C_i &= C_{i1}S_1 + C_{i2}S_2 \\ F_i &= C_{i1}f_1 + f_{i2}f_2 \end{aligned} \qquad i = 1 \text{ and } 2 \tag{50}$$

Equations 49 and 50 reflect the fact that, in this case,

$$C_{3,3} = 1 \text{ and } C_{1,3} = C_{2,3} = 0$$

For an immiscible gas flood, equations 49 and 50 together with equations 37 through 40 can be solved in a manner identical to the miscible algorithm with the exception that the phase equilibration calculations are performed on a two-phase normalized basis.

In this manner and according to the above assumptions, the total composition paths in solution space (as determined from the nonlinear method of characteristics) are solved from initial reservoir conditions to match with the set injection well conditions. During this process, the relative quantities of gas and liquid (total of oleic plus aqueous) phases are determined via fractional flow considerations, and the split of aqueous versus oleic phases is determined by a normalized two-phase flash calculation. A plot of F_i versus C_i reveals the nature of the solution process and demonstrates the existence of two distinct compositional paths, which together, represent

the solution for all composition values between initial and injection conditions.

Figure 9 shows an example of solution for F3 versus C3 (F3F - "fast path" through initial conditions, F3S - "slow path" through injection conditions) for a typical immiscible flood project with the characteristics listed in table 3. Also, shown here are the simulation results for the miscible model and the immiscible example runs based on the conditions in table 4.

The gas saturation (S3) remained constant throughout the calculations for the slow path. Under this condition, the nonlinear method of characteristics yields a consistent solution under the application of coherent wave theory. The fast path, which is based on initial conditions, is identical in the miscible and immiscible codes.

The slow path passes through the injection conditions, and these conditions are changed in the immiscible code to reflect the presence of three-phases. The following equations show the development of the injection conditions.

$$\text{Total injection rate} = Q_w + Q_{CO_2} = [\lambda_w + \lambda_g + \lambda_o]\nabla\phi|\text{sand face} \quad (51)$$

$$\frac{Q_w}{Q_{CO_2}} + 1 = [\lambda_w + \lambda_g + \lambda_o]\frac{\nabla\phi}{Q_{CO_2}} \quad (52)$$

or

$$WAG + 1 = [\lambda_w + \lambda_g + \lambda_o]\frac{\nabla\phi}{Q_{CO_2}} \quad (53)$$

where

$\nabla\phi$/sandface is the del function of porosity at the sandface of the well,

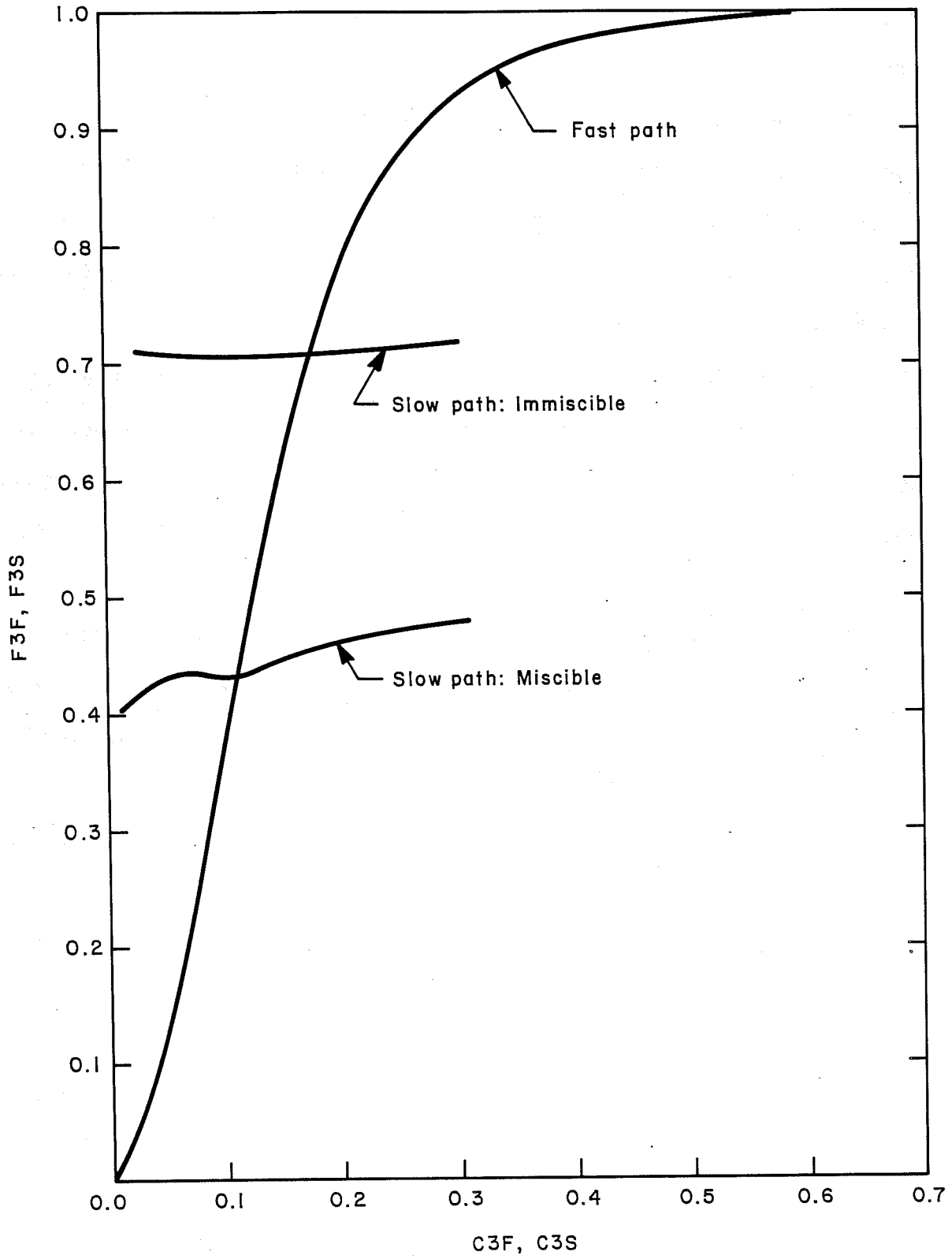

FIGURE 9. - Flux - compositional solution paths for a typical example CO_2 project.

TABLE 4. - Reservoir parameters and input conditions for test case study of the miscible and immiscible flood predictive model (MFPM) and (IFPM) - example run represents the Talco CO_2 flood

```
1
  ****************************************
  *              NPC  -  BETC            *
  *   CO2/MISCIBLE FLOOD PREDICTIVE MODEL  *
  *       (CO2PM - RELEASE 3.1.5)          *
  ****************************************

 TEST CASE - TALCO FIELD CO2 IMMISCIBLE FLOOD PROJECT

  CASE CONTROLS
  -------------
   RESERVOIR CALC METHOD ..............        1      IRES
+
   INTERMEDIATE OUTPUT ................       10      ICUT
   ACCOUNT FOR CO2/WATER SOLUBILITY ....       1      ISOL
   NUMBER OF LAYERS (NO CROSSFLOW) .....       1      LAYERS
C FORMATION PROPERTIES
  ----------------------
   FORMATION PRESSURE .................     484.0    PSIA
   FORMATION TEMPERATURE ..............     147.0    DEG.F
   POROSITY ...........................   0.2500     FRACTION
   NET THICKNESS (PAY) ................     200.0    FEET
   PATTERN AREA .......................      80.0    ACRES
   PERMEABILITY .......................     388.0    MD
   DEPTH ..............................    3785.0    FT
   VERT/HORIZ PERMEABILITY RATIO ......   0.1000     KV/KH
   RESERVOIR WATER SALINITY ...........  190000.     PPM
0 INITIAL CONDITIONS
  --------------------
   INITIAL OIL FRACTIONAL FLOW ........   0.0200     FRACTN
   PATH CONCENTRATION INCREMENT .......  0.010000    FRACTN
   RESERVOIR INJECTION RATE ...........     200.0    BBL/DAY



   INJECTED WAG RATIO .................      1.000    WATR/CO2
   HCPV OF CO2/WATER INJECTED (SLUG) ...    2.0000     HCPV
   MAX HCPV INJECTED (SLUG+CHASE) .....     4.0000     HCPV
   INITIAL AQUEOUS PHASE SATN .........     0.5606     FRACTN
   INITIAL OLEIC PHASE SATN ...........     0.4394     FRACTN
   WATER VISCOSITY ....................     1.0271     CP
+
   OIL VISCOSITY ......................    25.0000     CP
   CO2 VISCOSITY ......................     0.0170     CP
   WATER VOLUME FACTOR ................     1.0000     RB/STB
   OIL VOLUME FACTOR ..................     1.1000     RB/STB
   CO2 COMPRESSIBILITY FACTOR .........     0.8784     1/PSI
   CO2 VOLUME FACTOR ..................     3.7900     RB/MCF
   OIL GRAVITY ........................      23.00     DEG.API
   WATER DENSITY ......................     1.1167     G/CC
+
+


   CO2 DENSITY ........................     0.1532     G/CC
   CO2 DENSITY ........................        9.6     LB/CU.FT
   CO2 SOLUBILITY IN WATER ............       25.1     SCF/BBL
   OIL SOLUTION GAS CONTENT ...........      200.0     SCF/BBL
   INTERNAL DYKSTRA-PARSONS COEFF......     0.7000     VDP
1
```

TABLE 4. - Reservoir parameters and input conditions for test case study of the miscible and immiscible flood predictive model (MFPM) and (IFPM) - example run represents the Talco CO_2 flood (Continued)

RELATIVE PERM CURVES

OIL RELATIVE PERM CURVATURE	1.00
WATER RELATIVE PERM CURVATURE	1.00
OIL RELATIVE PERM END-POINT	0.900
WATER RELATIVE PERM END-POINT	0.500
IRREDUCIBLE WATER SATURATION	0.050
RESIDUAL OIL SATN AFTER WATER	0.300

RELATIVE PERMEABILITY TABLE

WATER SATURATN	OIL KRO	WATER KRW	FRACTION WATER	DERIV DFW/DSW
0.0500	0.9000	0.0000	0.0000	0.000
0.0825	0.8555	0.0055	0.4159	7.686
0.1150	0.8110	0.0110	0.6004	7.401
0.1475	0.7665	0.0165	0.7047	2.511
0.1800	0.7220	0.0220	0.7717	2.511
0.2125	0.6775	0.0275	0.8184	2.511
0.2450	0.6330	0.0330	0.8528	2.511
0.2775	0.5885	0.0385	0.8792	2.511
0.3100	0.5440	0.0440	0.9002	2.511
0.3425	0.4995	0.0495	0.9171	2.511
0.3750	0.4550	0.0550	0.9311	2.511
0.4075	0.4105	0.0605	0.9425	2.511
0.4400	0.3660	0.0660	0.9519	2.511
0.4725	0.3215	0.0715	0.9598	2.511
0.5050	0.2770	0.0770	0.9665	2.511
0.5375	0.2325	0.0825	0.9721	2.511
0.5700	0.1880	0.0880	0.9768	2.511
0.6025	0.1435	0.0935	0.9809	2.511
0.6350	0.0990	0.0990	0.9843	2.511
0.6675	0.0545	0.1045	0.9872	2.511
0.7000	0.0100	0.1100	0.9896	2.511
		0.1155	0.9916	2.511
		0.1210	0.9932	2.511
		0.1265	0.9945	2.511
		0.1320	0.9956	2.511
		0.1375	0.9964	2.511
		0.1430	0.9971	2.511
		0.1485	0.9976	2.511
		0.1540	0.9980	2.511
		0.1595	0.9983	2.511
		0.1650	0.9985	2.511
		0.1705	0.9987	2.511
		0.1760	0.9988	2.511
		0.1815	0.9989	2.511
		0.1870	0.9990	2.511
		0.1925	0.9991	2.511
		0.1980	0.9991	2.511
		0.2035	0.9992	2.511
		0.2090	0.9992	2.511
		0.2145	0.9993	2.511
		0.2200	0.9993	2.511
		0.2255	0.9993	2.511
		0.2310	0.9994	2.511
		0.2365	0.9994	2.511
		0.2420	0.9994	2.511
		0.2475	0.9994	2.511
		0.2530	0.9995	2.511
		0.2585	0.9995	2.511
		0.2640	0.9995	2.511
		0.2695	0.9995	2.511
		0.2750	0.9995	2.511
		0.2805	0.9995	2.511
		0.2860	0.9995	2.511
		0.2915	0.9996	2.511
		0.2970	0.9996	2.511
		0.3025	0.9996	2.511
		0.3080	0.9996	2.511
		0.3135	0.9996	2.511
		0.3190	0.9996	2.511
		0.3245	0.9996	2.511
		0.3300	0.9996	2.511
		0.3355	0.9996	2.511
		0.3410	0.9996	2.511
		0.3465	0.9996	2.511
		0.3520	0.9996	2.511
		0.3575	0.9996	2.511
		0.3630	0.9996	2.511
		0.3685	0.9996	2.511
		0.3740	0.9996	2.511
		0.3795	0.9996	2.511
		0.3850	0.9996	2.511
		0.3905	0.9996	2.511
		0.3960	0.9996	2.511
		0.4015	0.9996	2.511
		0.4070	0.9996	2.511
		0.4125	0.9996	2.511
		0.4180	0.9996	2.511
		0.4235	0.9996	2.511
		0.4290	0.9996	2.511
		0.4345	0.9996	2.511
		0.4400	0.9996	2.511
		0.4455	0.9996	2.511
		0.4510	0.9996	2.511
		0.4565	0.9996	2.511
		0.4620	0.9996	2.511
		0.4675	0.9996	2.511
		0.4730	0.9996	2.511
		0.4785	0.9996	2.511
		0.4840	0.9996	2.511
		0.4895	0.9996	2.511
		0.4950	0.9996	2.511
		0.5000	1.0000	0.000

and

$\lambda_{w,o,g}$ is the mobility of the water, oil, or gas.

During CO_2 injection;

$$Q_{CO_2} = \lambda_g \nabla\phi \tag{54}$$

then

$$WAG + 1 = 1 + \frac{\lambda_w}{\lambda_g} + \frac{\lambda_o}{\lambda_g} \tag{55}$$

or

$$WAG = \frac{\lambda_w}{\lambda_g} + \frac{\lambda_o}{\lambda_w}\frac{\lambda_w}{\lambda_g} \tag{56}$$

Finally

$$WAG = \frac{\lambda_w}{\lambda_g}\left(1 + \frac{\lambda_o}{\lambda_w}\right) \tag{57}$$

Now near the injection well, we assume that the reservoir is at or below residual oil saturation so that $\lambda_o = 0$.

$$WAG = \frac{\lambda_w}{\lambda_g} \equiv \text{injection condition} \tag{58}$$

Define

$$FUNC = WAG - \frac{\lambda_w}{\lambda_g} = 0 \tag{59}$$

Expanding λ_w and λ_g in terms of effective permeability and viscosity:

$$FUNC = WAG - \frac{V(3)}{V(1)} \frac{KR1E}{KR3E} \frac{\left[\frac{S1-S1R}{1-S1R-S2R-S3R}\right]^M}{\left[\frac{S3-S3R}{1-S1R-S2R-S3R}\right]^{MN}} = 0 \tag{60}$$

Imposing the constraint:

$$S1+S2R+S3 = 1$$

$$FUNC = WAG - \frac{V(3)}{V(1)} \frac{KR1E}{KR3E} \frac{\left[\frac{1-S2R-S3-S1R}{1-S1R-S2R-S3R}\right]^M}{\left[\frac{S3-S3R}{1-S1R-S2R-S3R}\right]^{MN}} = 0 \tag{61}$$

This equation is solved iteratively for the variable S3 using the Bisection algorithm. The solution algorithm is presented in the next section.

D. Description of Code Changes and Flow Diagram of Modifications

In SUBROUTINE INPUT, eight new parameters are read in. These are:

THETA = dip angle (radians)

G = gravitational acceleration (cm/sec^2)

RHO1 = water density (gm/cm^3)

RHO2 = oil density (gm/cm^3)

RHO3 = CO_2 density (gm/cm^3)

XKRGE = end-point gas relative permeability

SORG = residual gas saturation

XNG = exponent for gas saturation function

Also, in SUBROUTINE INPUT, the scheme which calculates the initial phase saturations and concentrations injected was replaced with a new iteration scheme based on the Bisection Method which takes into account the presence of three phases. An inherent assumption in this iteration scheme is that the reservoir is swept to residual oil saturation near the injection well. Under this assumption S2 → S2R and S1 → 1-S2R-S3. Thus, only the gas saturation needs to be determined in this iteration method. The complete Bisection algorithm is given in appendix C. S1PI, S2PI, and S3PI in appendix C are transferred in common to SUBROUTINE PATH where they are used to calculate the initial injected concentrations along the slow path.

In SUBROUTINE FRACT a modification was made to allow specification of S3 before SUBROUTINE PATH is called. The modification is given in appendix D. S(3) is in common with SUBROUTINE PATH and S31 is in common with SUBROUTINE INPUT where it is calculated using the bisection algorithm.

In SUBROUTINE PATH the three-phase saturations calculated by the bisection algorithm in SUBROUTINE INPUT are renormalized to two-phase values. This is done only along the slow path (IPTH=-1). The renormalization is as follows:

```
S1NPI = S1PI/(1.-S3PI)
S2NPI = S2PI/(1.-S3PI)
```

These saturations are then used to calculate the initial injected concentrations given by:

```
CTP2  = 1.E-6
CTP3  = (1.-XK(1))*(S1NPI+XK(3)*S2NPI)/(XK(3)-XK(1))
```

where the XK(I) are K-values.

This calculation is made only during the first iteration through the slow path loop. For subsequent iterations, we set C2=CTP2 and C3=CTP3. These concentrations are then used in calling SUBROUTINE FLASH where new two-phase

saturations are calculated. These saturations (SFP1,SFP2) are then expanded to three-phase values as follows:

```
RPF   = SFP1/SFP2
S(2)  = (1.0-S(3))/(1.0+RPF)
S(1)  = RPF*S(2)
```

Throughout these calculations S(3) remains constant. SUBROUTINE FLOW is then called to calculate the fluxes which are based on fractional flow and hence three-phase saturations.

This series of calculations is performed with unperturbed concentrations and then after each perturbation for numerical derivatives along the solution path in the slow path loop.

In SUBROUTINE FLOW the relative permeability treatment was modified to account for the presence of three phases. The saturation functions were expanded first as follows:

```
SF1   = (S(1)-S1R)/(1.-S1R-S2R-S3R)
SF2   = (S(2)-S2R)/(1.-S1R-S2R-S3R)
SF3   = (S(3)-S3R)/(1.-S1R-S2R-S3R)
```

where S1R, S2R, S3R = water, oil, gas residual saturations, respectively. The relative permeabilities are then calculated as:

```
KR1   = KR1E*SF1**M
KR2   = KR2E*SF2**N
KR3   = KR3E*SF3**MN
```

where KR1E, KR2E, KR3E = water, oil, gas end point relative permeabilities and M,N,MN = experimentally determined exponents.

The fractional flow calculations were then expanded to include three phases and the effect of reservoir dip. First the parameter RKADQ was defined as:

```
      RKADQ = (0.49828E-6)*SQRT(43560.*AREA)*THICK/QRES
```

The fractional flow of water was then expressed as:

```
      FF1   = (1.-(KR2*RKADQ/V2)*(RHO1-RHO2)*G*SIN(THETA)
     1 -(KR3*RKADQ/V(3))*(RHO1-RHO3)*G*SIN(THETA))
     2 /(1.+(V1/V2)*(KR2/KR1)+(V1/V(3))*(KR3/KR1))
```

The fractional flow of oil was expressed as:

```
      FF2   = (1.-(KR3*RKADQ/V(3))*(RHO2-RHO3)*G*SIN(THETA)
     1 +(KR1*RKADQ/V1)*(RHO1-RHO2)*G*SIN(THETA)
     2 /(1.+(V2/V1)*(KR1/KR2)+(V2/V(3))*(KR3/KR2))
```

The fractional flow of gas is then calculated by difference:

```
      FF3   = 1.0-FF2-FF1
```

The fluxes are also calculated in SUBROUTINE FLOW. The CO_2 flux, FLX3, was modified to include the fractional flow of gas in the following manner:

```
      FLX3 = C(3,1)*FF1+F2(3)*FF2+FF3
```

A flow diagram showing these modifications is presented in figure 10.

E. Discussion of Test Cases and Sensitivity Analysis of Modified Code

A direct comparison of the miscible CO_2 flood predictive model (MFPM) with the immiscible CO_2 flood predictive model (IFPM) was made using data from the Talco CO_2 flood project. The basic input data to these models are presented in table 4.

Using these data, a comparison of the resulting oil rate versus time for the two models is given in figure 11. The oil rates before CO_2 breakthrough are identical (5.5 BOPD). After CO_2 breakthrough, the oil rate drops to 2.4 BOPD using the miscible code and remains constant throughout the project life. Using the immiscible code, the oil rate drops sharply to 0.1 BOPD after

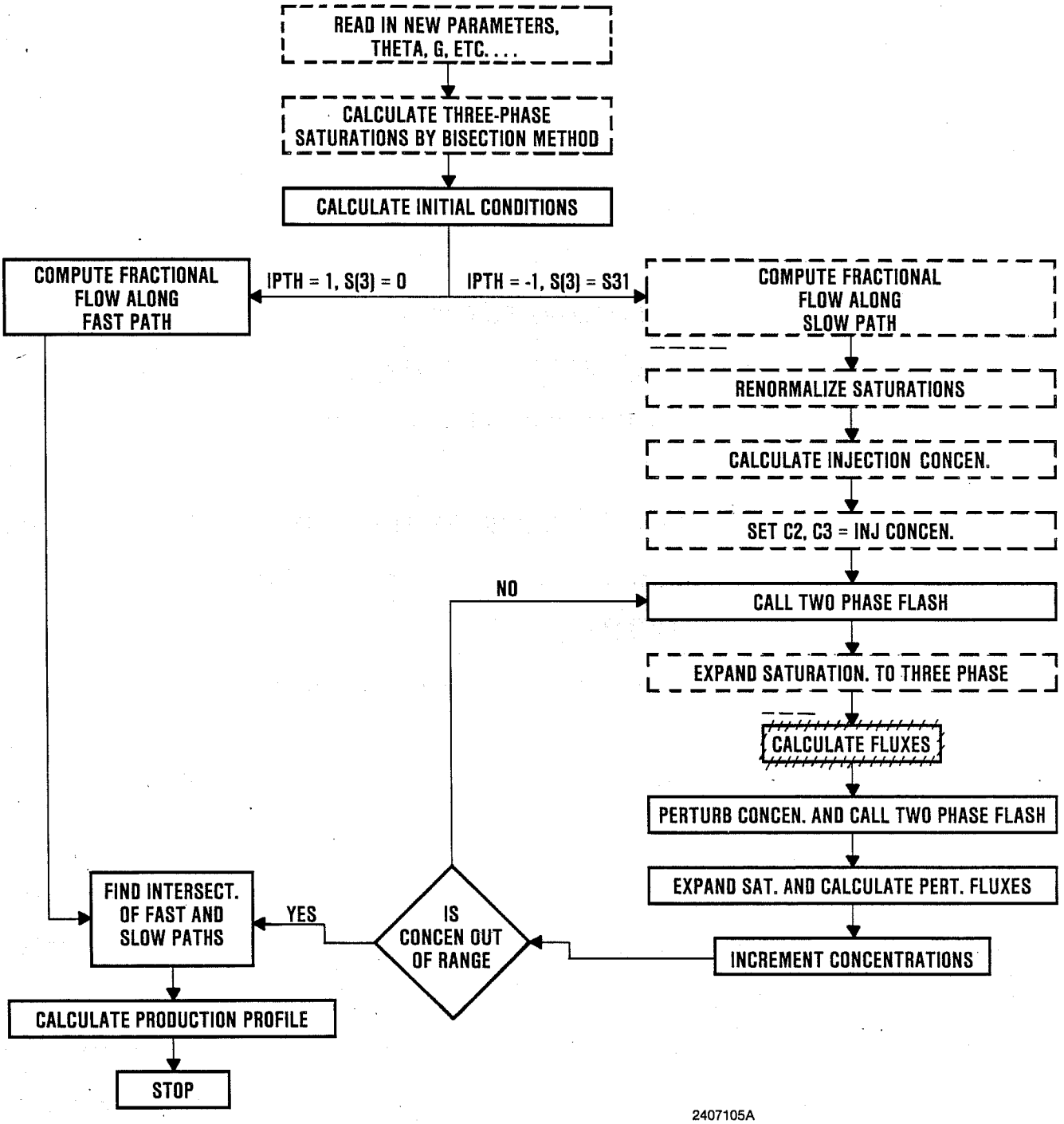

FIGURE 10. - Logic flow diagram of Program IFPM showing changes to MFPM. Dotted boxes indicate changes and additions.

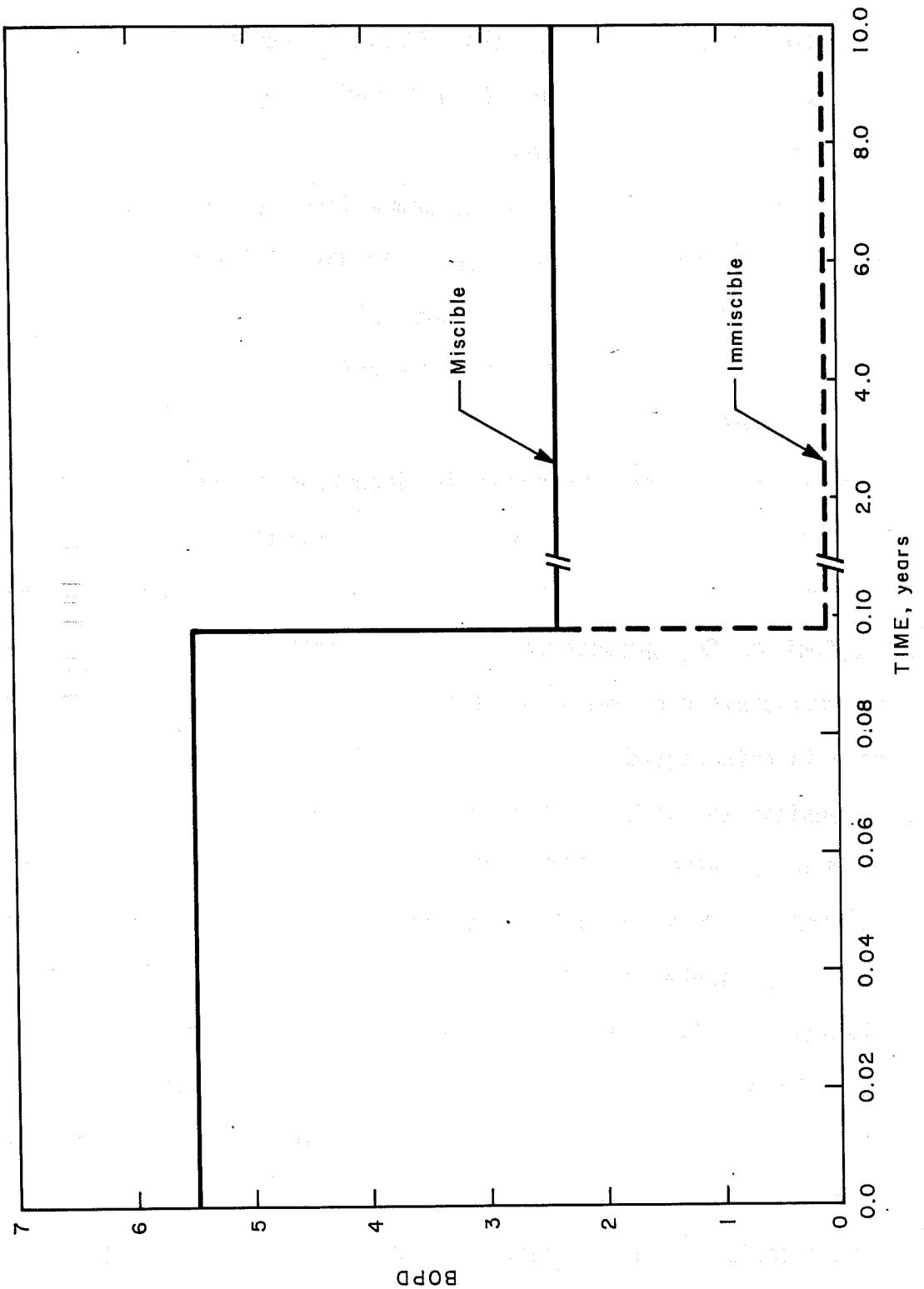

FIGURE 11. - Oil production rate history (MFPM and IFPM).

CO_2 breakthrough and remains constant throughout the project life. The lower oil rate for the immiscible code is consistent with expectations since immiscible displacements are generally less effective than miscible displacements. After gas breakthrough, high CO_2 mobility with oil near residual saturation results in very low oil rates.

For this same set of computer runs, a comparison of the resulting CO_2 production rates is presented in figure 12. The CO_2 production rate after breakthrough is significantly higher in the immiscible code output compared to the miscible. This result is due largely to the presence of a free gas saturation in the immiscible calculations.

A sensitivity study was then conducted to determine the effect of reservoir dip angle on production for MFPM and IFPM. No effect on oil production rate was found using either code for dip angles up to 45°. However, there was a significant effect on CO_2 production rate after breakthrough, as shown in figure 13. The immiscible code was more sensitive to reservoir dip angle than the miscible code in this regard.

Finally, a sensitivity study was conducted to determine the effect of WAG ratio on production for MFPM and IFPM. WAG ratios of 0.5, 1.0 (base case), and 2.0 were tested. A plot of oil production rate after CO_2 breakthrough versus WAG ratio is presented in figure 14. It is clear that IFPM is more sensitive to WAG ratio, with regard to oil rate, than MFPM especially in the region above a WAG ratio of 1.0. However, as figure 15 shows, CO_2 production falls rapidly as WAG increases for the miscible case, while CO_2 production is relatively constant in the immiscible case, showing the miscible sensitive to WAG ratio. In this case, it appears that lower gas (solvent) fractional flows at higher WAG ratios permit higher oil fractional flows.

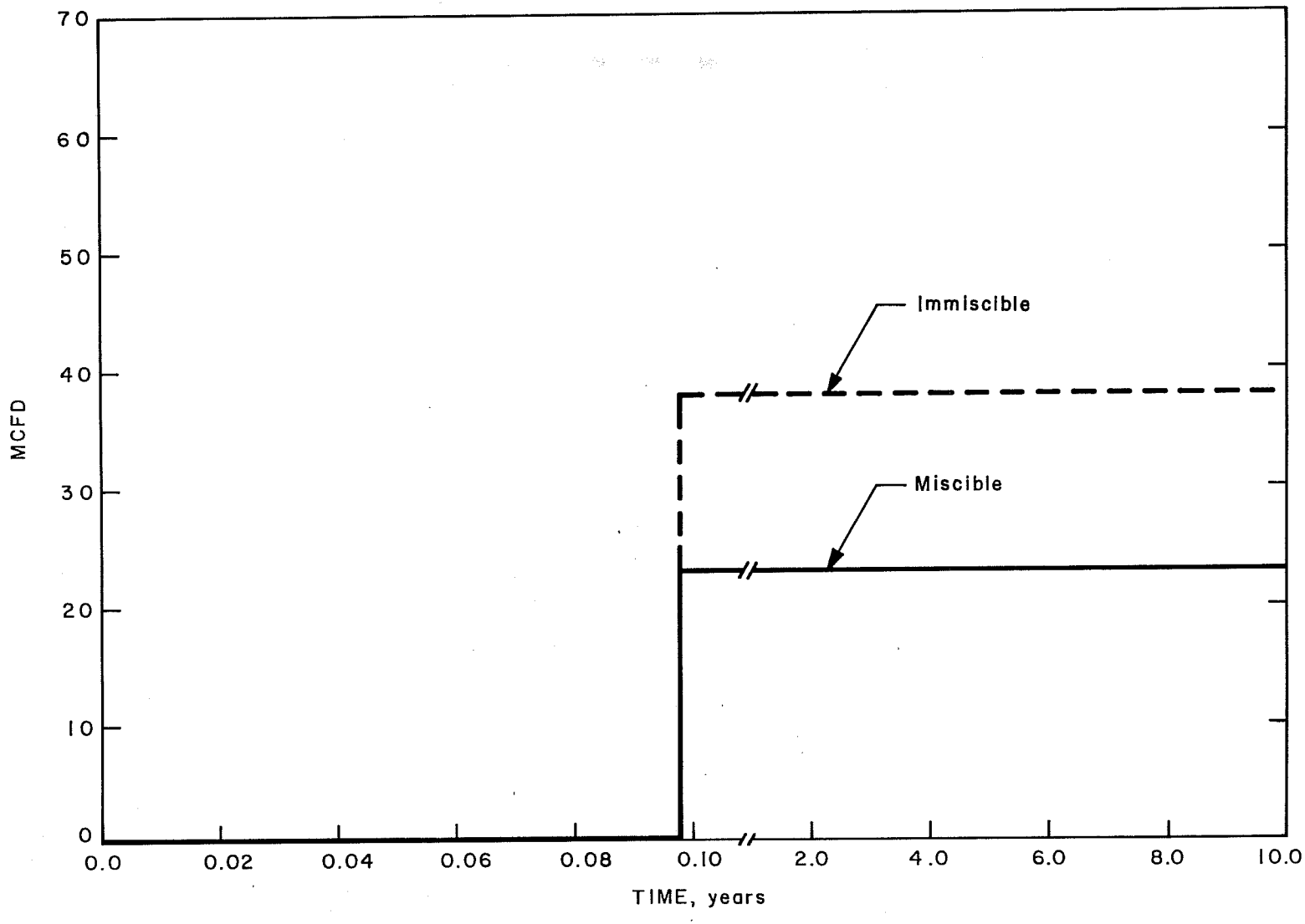

FIGURE 12. - CO_2 production rate history.

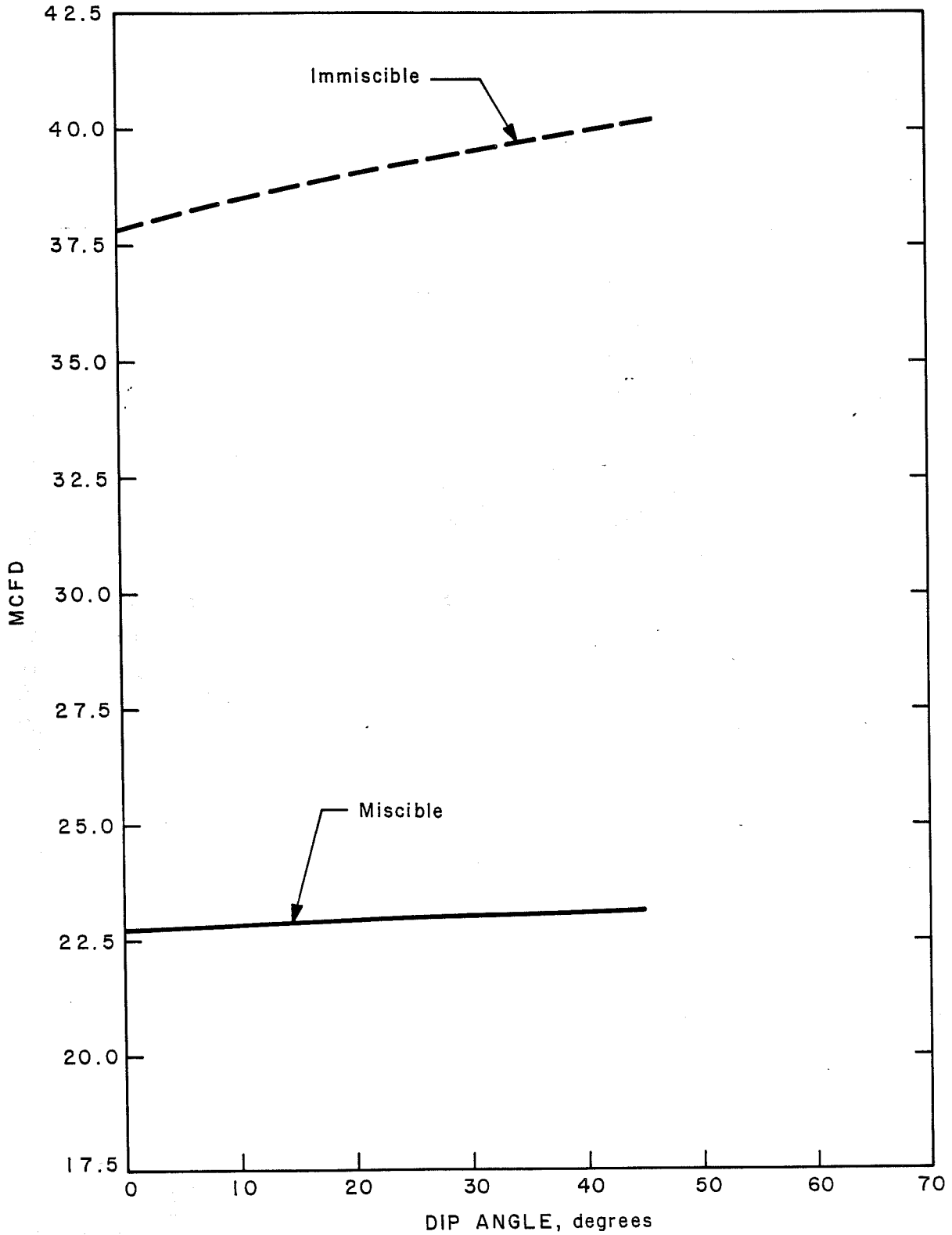

FIGURE 13. - Sensitivity of CO_2 production rate for various DIP angles.

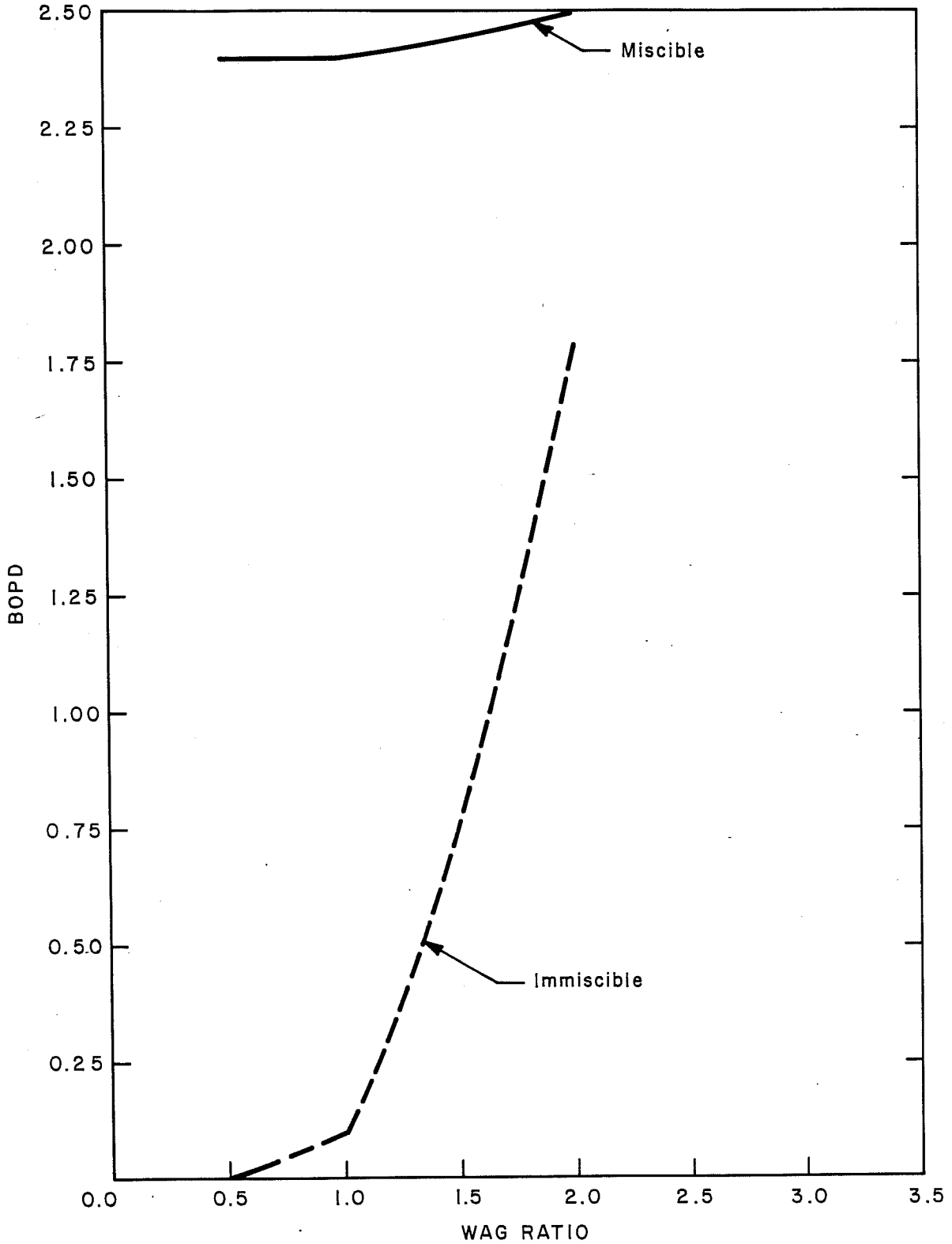

FIGURE 14. - Sensitivity of oil production (after CO_2 breakthrough) to WAG ratio.

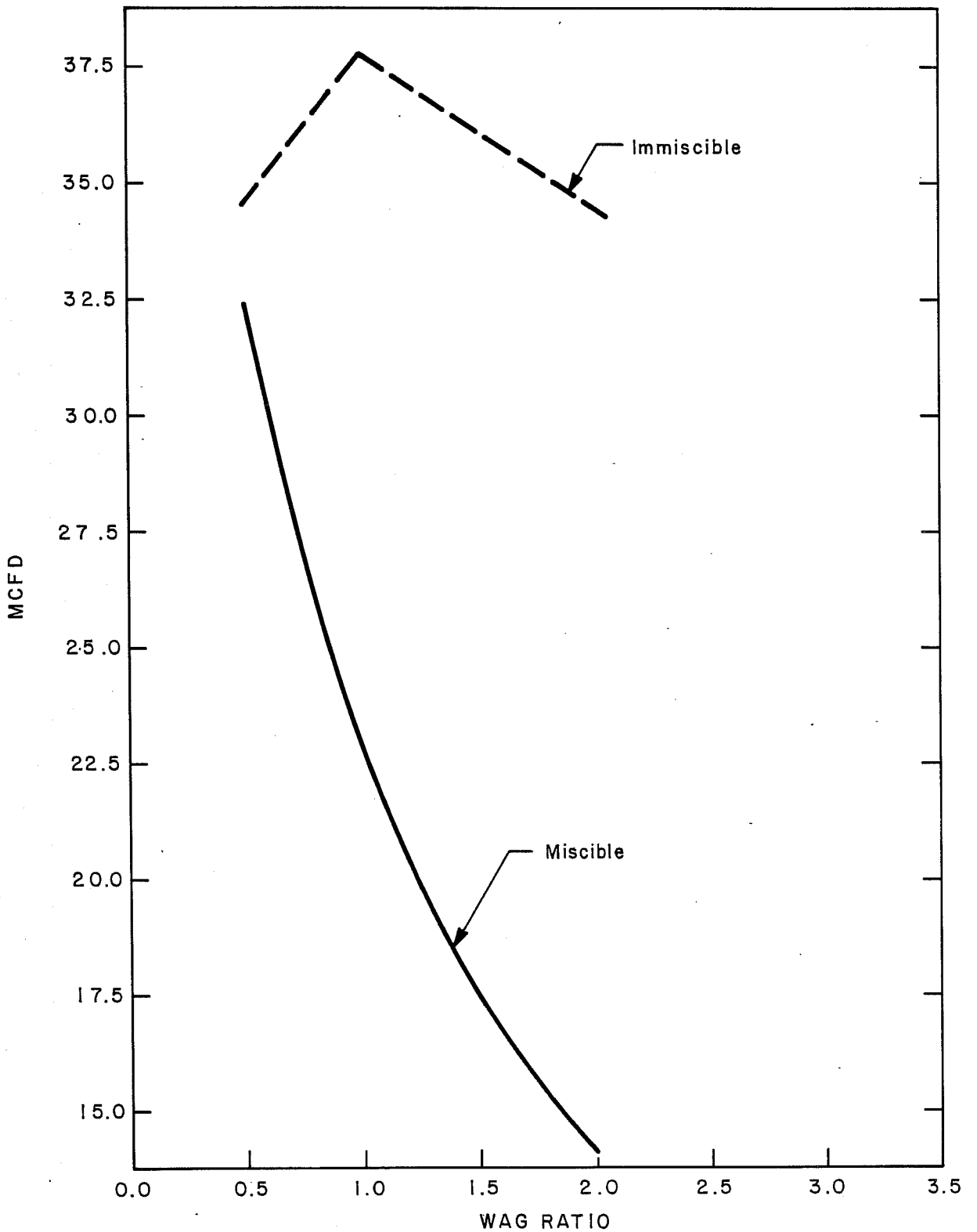

FIGURE 15. - Sensitivity of CO_2 production rate (after breakthrough) to WAG ratio.

F. Field Test Comparison of Modified CO_2 Predictive Models

F.1 CO_2 (Miscible) Predictive Model Modified to Include Reservoir Dip

As discussed in Section E, the sensitivity of production rates to dip angle in the miscible predictive model is negligible; see figure 13. This version of the model (without dip) has already been calibrated during the recent NPC EOR potential study. A documented (annotated) listing of the CO_2 miscible model with formation dip is supplied to DOE/BPO. The code is now called CO2DIP.

The reservoir site selected to test the CO_2 miscible predictive model with dip is the Slaughter Estate pilot unit consisting of 13.2 acres in the midst of a 5,704-acre reservoir. The base case values and term definitions are shown in table 5. The base values are essentially those used in the final report DOE/BC/10327-20.[7] Waterflooding in the Slaughter Unit began in 1963, and a CO_2 pilot began in November 1972, with water injection continuing until August 1976, when the CO_2 acid gas injection was begun. All of the related reservoir parameters used in the miscible predictive model sensitivity study are shown in table 6, columns 2 and 3.

Results from the use of the CO_2 predictive model match the production history of the Slaughter Estate pilot very well as long as one layer is used and the Dykstra-Parsons coefficient is 0.25, also an oil curvature (XNO) of 2.4 is slightly better than 2.55. Table 7 shows the comparison between the production history of the 12-acre pilot and the prediction of the model for one, three, and five layers with a VDPL of 0.48. The production history is from available literature.[8] Figure 16 shows the match between predicted cumulative oil and the Slaughter pilot history assuming one layer.

TABLE 5. - Base values for Slaughter Estate pilot unit

Variable name	Description	Base value	Units
PRES	Reservoir pressure	2000	psig
TRES	Reservoir temperature	105	deg. F
POROS	Reservoir porosity	0.113	fraction
THICK	Net pay thickness	77.5	feet
AREA	Pattern area	12.29	acres
PERM	Reservoir absolute permeability	6	Md
DEPTH	Reservoir depth	5,000	feet
XKVH	Vertical to horizontal permeability ratio	0.01	fraction
SALN	Water salinity	50,000	ppm
BO	Oil formation volume factor	1.22	bbl/stb
RS	Solution gas-oil ratio	600	scf/stb
BW	Water formation volume factor	1.0	bbl/stb
BCO2	CO_2 formation volume factor	0.4	bbl/mscf
API	API gravity of oil	28	deg. API
SGG	Specific gravity of gas (air = 1)	0.8	fraction
FOINIT	Initial oil cut at CO_2 flood start	0.13	fraction
DELTR	Time increment for recovery calculations	0.5	years
DELC3	Concentration increment for fractional flow calculations	0.001	fraction
QRES	Total reservoir injection rate	390	bbl/day
WAG	Water/Gas ratio for CO_2 injection	1	
HPVWSI	Total hydrocarbon pore volumes of CO_2 and water injected	1	
PVMAX	Total pore volumes of WAG and Chase volumes	4	
VWAT	Water viscosity at reservoir conditions	0.8023	cps
VOIL	Oil viscosity at reservoir conditions	2.	cps
VISC	CO_2 viscosity at reservoir conditions	0.074	cps
VDP	Dykstra-Parsons coefficient for reservoir heterogeneity	0.25	fraction
VDPL	Dykstra-Parsons coefficient for reservoir heterogeneity for use between layers	0.48	fraction
XNO	Exponent for oil relative permeability curve	2.55	
XNW	Exponent for water relative permeability curve	1.78	
XKROE	Relative permeability to oil at connate water saturation	1.0	
XKRWE	Relative permeability to water at residual oil saturation	0.34	
SWCN	Connate water saturation	0.08	fraction
SORW	Residual oil saturation to water ratio	0.31	fraction
THETA	Reservoir dip angle	0.4	deg.
RHO1	Specific gravity of water	1.0265	fraction
RHO2	Specific gravity of oil	0.823	fraction
RHO3	Specific gravity of solvent	0.7709	fraction

TABLE 6. - Results of sensitivity study for Slaughter Estate unit

Variable name	Base change		Peak rate of oil STB/d (Base=133.2)		Time of peak, years (Base=2.01)		Maximum for cumulative oil, MSTB (Base=225.4)		Time to reach maximum cumulative oil/ years (Base=8.51)	
	-20%	+20%	-20%	+20%	-20%	+20%	-20%	+20%	-20%	+20%
PRES	1600	2400	134.6	131.8	2.02	2.01	225.0	224.0	8.52	8.51
TRES	84	126	135.6	138.4	2.02	2.03	225.3	227.2	9.02	9.03
POROS	0.0904	0.1356	123.0	156.9	1.81	2.21	177.1	263.4	6.81	10.21
THICK	62	93	123.1	149.7	1.81	2.22	177.2	262.1	6.81	10.22
AREA	9.83	14.75	123.1	152.6	1.81	2.22	177.1	262.6	6.81	10.22
PERM	4.8	7.2	133.1	133.4	2.01	2.01	224.4	224.5	8.51	8.51
DEPTH	4000	6000	133.2	133.2	2.01	2.01	224.4	224.4	8.51	8.51
XKVH	0.008	0.012	133.2	133.2	2.01	2.01	224.4	224.4	8.51	8.51
SALN	4000	6000	132.2	134.3	2.01	2.02	224.1	224.8	8.51	8.52
BO	0.98	1.46	165.8	111.3	2.01	2.01	279.4	187.5	8.51	8.51
RS	480	720	133.2	133.2	2.01	2.01	224.4	224.4	8.51	8.51
BW	0.8	1.2	133.2	133.2	2.01	2.01	224.4	224.4	8.51	8.51
BCO2	0.32	0.48	133.2	133.2	2.01	2.01	224.4	224.4	8.51	8.51
API	22.4	33.6	133.2	133.2	2.01	2.01	224.4	224.4	8.51	8.51
SGG	0.64	0.96	133.2	133.2	2.01	2.01	224.4	224.4	8.51	8.51
FOINIT	0.104	0.156	131.8	134.8	2.05	1.99	204.1	230.5	8.55	8.49
DELTR	0.4	0.6	144.1	125.4	1.81	2.21	218.7	224.8	8.61	8.81
DELC3	0.0008	0.0012	138.3	137.4	2.03	2.03	225.4	225.1	8.53	8.53
QRES	312	468	112.6	150.7	2.27	1.84	217.7	225.4	10.77	7.34
WAG	0.8	1.2	135.3	123.7	1.99	2.06	232.6	216.3	8.49	8.56
HPVWSI	0.8	1.2	133.2	133.2	2.01	2.01	209.7	237.7	7.51	9.51
PVMAX	3.2	4.8	133.2	133.2	2.01	2.01	224.4	224.4	8.51	8.51
VWAT	0.6418	0.9628	136.9	134.4	2.06	1.99	234.5	221.4	9.06	8.49
VOIL	1.6	2.4	129.8	138.0	2.03	2.02	217.5	235.7	8.53	9.02
VISC	0.059	0.089	133.2	129.4	1.98	2.05	213.8	223.8	8.98	8.55
VDP	0.2	0.3	136.5	124.5	2.05	1.99	220.1	214.1	9.05	8.99
XNO	2.04	3.06	127.4	118.3	2.06	1.97	199.0	237.5	11.56	9.47
XNW	1.42	2.14	130.1	125.1	2.08	1.97	220.2	217.7	9.08	8.47
XKROE	0.8	1.2	135.5	136.0	2.04	2.01	236.5	221.8	9.04	8.51
XKRWE	0.272	0.408	129.2	138.2	1.98	2.05	219.4	234.8	8.48	9.05
SWCN	0.064	0.096	131.1	135.4	2.03	2.00	227.5	222.5	9.03	8.50
SORW	0.248	0.372	126.5	116.0	2.55	1.47	219.4	212.0	9.05	7.97
THETA	0.32	0.48	133.1	133.3	2.01	2.01	224.4	224.4	8.51	8.51
RHO1	0.8212	1.2318	132.5	134.1	2.00	2.02	211.2	224.6	8.50	8.52
RHO2	0.6584	0.9876	133.9	132.7	2.02	2.00	224.5	224.4	8.52	8.50
RHO3	0.6167	0.9251	133.2	133.2	2.01	2.01	224.4	224.4	8.51	8.51

TABLE 7. - Predictive model simulation and history match of CO_2 recovery for Slaughter Estate Unit, Hockley County, Texas. VDPL = .48

	Layers	Peak rate of oil, STB/d	Time of peak, years	Maximum for cumulative oil, MSTB	Time to reach maximum cumulative oil/ years
Production history	--	143	2.25	>170	>5.0
	1	133.2	2.01	224.4	8.51
	3	101.5	1.13	221.2	13.15-
	5	97.6	1.34	223.6	15.18

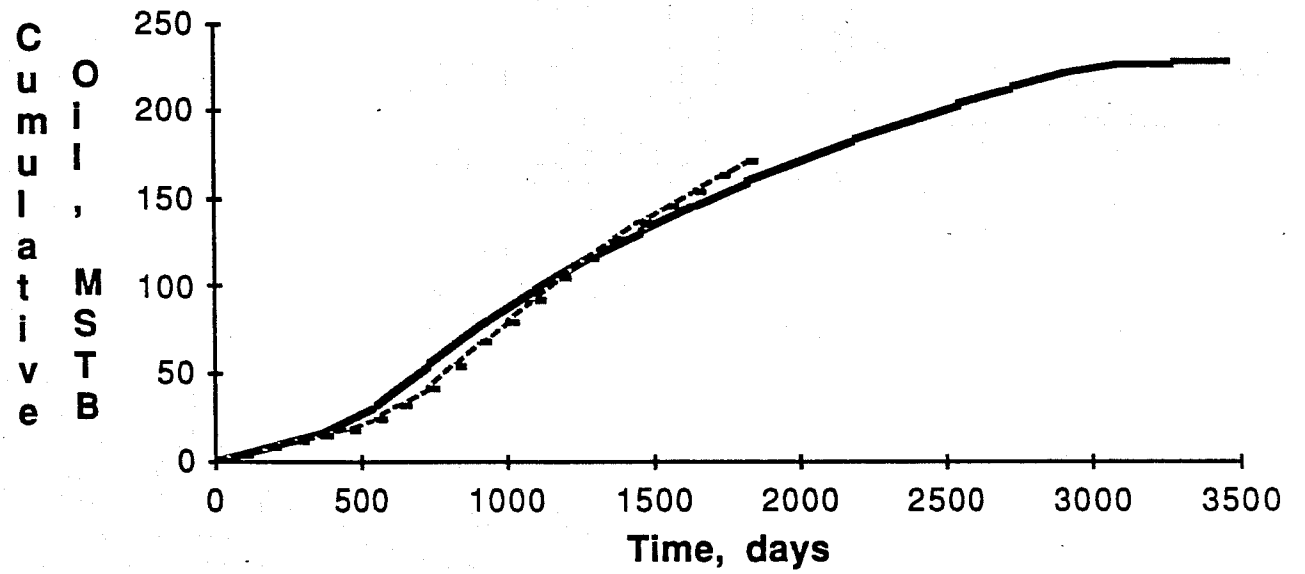

Figure 16. History match of MFPM (3D) for Slaughter Estate Pilot Field (1 Layer). (Solid curve is predicted.)

F.2 CO_2 Immiscible Predictive Model Comparison

A reservoir site selected to test field data against the immiscible predictive model is the Talco field consisting of 240 acres in the mid-continent region of Texas. Producing out of the Paluxy formation, tertiary recovery was begun in May 1982 under an immiscible non-hydrocarbon gas displacement method. Although the project evaluation was discouraging, the total production reached 462 bbl oil per day, none of which was established as enhanced production. The immiscible predictive model was tested on an 18.5-acre pattern in the test field. No production history was available for comparison. Field values chosen for the tests are shown later in table 8. A documented listing of the CO_2 immiscible predictive model is supplied to DOE/BPO. The code is now called CO2IMMIS.

F.3 Results of Field Test Sensitivity Studies

The sensitivity study included in this report shows the resulting oil production rate and cumulative oil production when one selected variable is changed by an appropriate amount in either direction from the normal. The normal is the base set of variable values which optimized the known field data and production history of the particular reservoir selected.

There are nine variables which appear to have no effect on the results from the base data as input. These variables are for all practical purposes, decoupled for this base, and they are DEPTH, XKVH, RS, BW, BCO2, API, SGG, PVMAX, and RHO3. They are either not used because defaults of other variables are not needed or because the base data are out of the range where they are needed. Three other variables appear to have a negligible effect with the

TABLE 8. - Base values for Talco field, CO_2 immiscible flood project

Variable name	Base value	Variable name	Base value
PRES	484	HPVWSI	2
TRES	147	PVMAX	4
POROS	0.25	VWAT	1.0
THICK	200	VOIL	25
AREA	18.5	VISC	0.017
PERM	388	VDP	0.7
DEPTH	3785	VDPL	0.7
XKVH	0.1	LAYERS	1
SALN	190000	XNO	1
BO	1.1	XNW	1
RS	200	XKROE	0.9
BW	3.79	XKRWE	0.5
BCO2	3.79	SWCN	0.05
API	23	SORW	0.3
SGG	0.7	THETA	0.0
FOINIT	0.02	RHO1	1
DELTR	0.5	RHO2	0.916
DELC3	0.01	RHO3	0.061
QRES	200	XKRGE	0.5
WAG	1		

base used and are PERM, SALN, and THETA. THETA variations actually do not begin to have a large effect until above 40 degrees when using the Slaughter base.

The largest changes in peak rates are made by changes in BO, QRES, POROS, AREA, and THICK, in that order. Except for QRES, the same changes occur in cumulative oil. The most sensitive variable is BO.

Although the effect of reservoir temperature is very small it is unusual in that a 20-percent decrease causes small increases in peak rate and cumulative production, whereas a 20-percent increase causes slightly larger increases. These changes are small, and actual causes are not known but may be artifacts of the model.

Other peculiar reversals show up with DELC3, VISC, XNO, XNW, XKROE, and SORW, in regard to oil rate of cumulative oil. DELC3 actually begins to decrease the peak oil rate substantially when its value moves from 0.01 to 0.1.

Although 20-percent variations of the dip (THETA) have a negligible effect on the Slaughter base data results, a change of THETA from 10 to 30 degrees of dip will lower the oil production rate 1.2 percent at a permeability value of 6 md, 7.1 percent at 60 md, and 13.0 percent at 120 md. These results are shown in table 9 for one layer and VDP = 0.48.

Table 10 shows a list of 20 variables which are the most sensitive resulting in altering either the peak oil rate or the cumulative oil production in an order of decreasing sensitivity. The percentage of change to either the peak rate or to cumulative oil is shown alongside the variable affecting the change. The percentage of change reflects the total range of variation of -20 to +20 percent for each variable.

TABLE 9. - Relationship between dip angle (THETA) and permeability for Slaughter Estate pilot unit

Permeability, md	Peak rate, STB/D	Time step of peak, years	Maximum cumulative oil, MSTB
		THETA = 10	
6	75.8	3.39	213
60	70.1	3.34	207
120	66.8	3.29	204
		THETA = 30	
6	74.9	3.38	214
60	65.1	3.79	206
120	58.1	3.70	197

TABLE 10. - Sensitivity of variables to Slaughter Estate base case (Percent change for the variable range of -20 to +20 percent of base value)

Oil rate change		Cumulative oil change	
Variable	Percent	Variable	Percent
BO	-40.9	BO	-41.0
QRES	28.6	POROS	38.5
POROS	25.5	AREA	38.1
AREA	22.1	THICK	37.8
THICK	20.0	XNO	17.2
DELTR	-14.0	HPVWSI	12.5
WAG	-9.0	FOINIT	11.8
VDP	-9.0	VOIL	8.1
SORW	-7.9	WAG	-7.3
XNO	-6.8	XKRWE	6.9
XKRWE	6.8	XKROE	-6.6
VOIL	6.2	RHO1	6.0
XNW	-3.8	VWAT	-5.8
SWCN	3.2	VISC	4.4
VISC	-2.9	SORW	-3.3

All other variables result in changes of less than 2.9 percent. As would be expected, the large changes of production are made with porosity, area, formation thickness, and volume factor, and the injectivity QRES changes the oil rate and peak time but not the cumulative oil so much. On the other hand, the slug size (HPVWSI), oil curvature (XNO), and the oil cut (FOINIT) have more effect on the cumulative oil production than on the oil rate. Actually, XNO has the opposite effect on oil rate.

A sensitivity study, similar to that of the Slaughter Estate, was made on Talco field using the CO_2 immiscible predictive model CO2IMMIS (IFPM). Table 8 presents the Talco field base case values for the variables using the same detinitions as with Slaughter field. Table 11 shows the resulting oil rates and cumulative oil productions. Table 12 indicates the variables most sensitive to changing oil rate or cumulative oil. The area, porosity, and thickness do not affect the oil rate in the immiscible model run on Talco field as they do in the dipped miscible model run on Slaughter field. Also, the shape of the oil rate and cumulative oil curves are very different in the two models.

Special indirect command files (CSS) and CO_2 predictive model data input, data editing, and graphic output display programs were used to conduct the sensitivity studies for the immiscible and miscible with dip models. Listing of these programs and indirect command files are also supplied to DOE/BPO.

TABLE 11. - Talco field, CO_2 immiscible flood project

Variable name	Base change		Peak rate of oil STB/d (Base=5.38)		Time of peak, years (Base=14.54)		Maximum for cumulative oil, MSTB (Base=49.77)		Time to reach maximum cumulative oil/ years (Base=50.04)	
	-20%	+20%	-20%	+20%	-20%	+20%	-20%	+20%	-20%	+20%
PRES	387.2	580.8	5.38	5.38	15.12	15.12	52.33	51.00	50.13	50.12
TRES	117.6	176.4	5.38	5.38	14.52	14.67	49.66	49.99	50.02	50.17
POROS	.2	.3	5.38	5.38	11.63	17.45	43.32	56.03	50.13	50.45
THICK	160	240	5.38	5.38	11.63	17.45	43.32	56.03	50.13	50.45
AREA	14.8	22.2	5.39	5.38	11.82	18.08	43.85	57.31	50.32	50.08
PERM	310.4	465.6	5.39	5.38	14.78	15.07	50.64	50.74	50.28	50.07
DEPTH	3028	4542	5.38	5.38	14.54	14.54	49.77	49.77	50.04	50.04
XKVH	.08	.12	5.39	5.38	14.78	15.07	50.64	50.74	50.28	50.07
SALN	152000	228000	5.38	5.38	15.48	15.16	52.19	51.19	50.48	50.16
BO	.88	1.32	6.73	4.48	14.54	14.54	62.21	41.47	50.04	50.04
RS	160	240	5.38	5.38	14.54	14.54	49.77	49.77	50.04	50.04
BW	.8	1.2	5.38	5.38	14.54	14.54	49.77	49.77	50.04	50.04
BCO2	3.032	4.548	5.38	5.38	14.54	14.54	49.77	49.77	50.04	50.04
API	18.4	27.6	5.38	5.38	14.54	14.54	49.77	49.77	50.04	50.04
SGG	.56	.84	5.38	5.38	14.54	14.54	49.77	49.77	50.04	50.04
FOINIT	.016	.024	4.65	6.12	15.37	13.69	45.71	53.32	50.37	50.19
DELTR	.4	.6	5.38	5.38	14.54	14.54	49.78	49.93	50.14	50.54
DELC3	.008	.012	5.38	5.38	14.88	14.59	50.80	49.87	50.38	50.09
QRES	160	240	4.30	6.46	19.42	12.59	48.12	54.78	50.42	50.09
WAG	.8	1.2	5.38	5.38	12.91	17.25	45.31	56.51	50.41	50.25
HPVWSI	1.6	2.4	5.38	5.38	14.54	14.54	49.77	49.76	50.04	50.04
PVMAX	3.2	4.8	5.38	5.38	14.54	14.54	49.77	49.77	50.04	50.04
VWAT	.82168	1.23252	5.37	5.38	12.84	12.84	45.48	52.80	50.34	50.14
VOIL	20	30	5.37	5.39	15.14	14.29	51.67	48.63	50.14	50.29
VISC	.0136	.0204	5.39	5.37	15.64	14.05	52.45	48.73	50.14	50.05
VDP	.56	.84	5.47	5.16	15.20	14.38	54.78	45.61	50.20	50.38
XKROE	.72	1.08	5.40	5.36	12.57	16.12	44.66	53.77	50.07	50.12
XKRWE	.4	.6	5.36	5.40	16.47	13.68	54.81	47.53	50.47	50.18
SWCN	.04	.06	5.38	5.38	15.05	14.80	50.71	50.59	50.05	50.30
SORW	.24	.36	5.36	5.41	13.81	16.36	47.94	54.25	50.31	50.36
RHO1	.8	1.2	5.38	5.38	14.54	14.54	49.77	49.77	50.04	50.04
RHO2	.7328	1.0992	5.38	5.38	14.54	14.54	49.77	49.77	50.04	50.04
RHO3	.0488	.0732	5.38	5.38	14.54	14.54	49.77	49.77	50.04	50.04
XKRGE	.4	.6	5.38	5.38	15.38	14.65	51.85	50.14	50.38	50.17

TABLE 12. - Sensitivity of variables to Talco field base case

Oil rate change		Cumulative oil change	
Variable	Percent	Variable	Percent
BO	-41.8	BO	-41.7
QRES	40.1	AREA	27.1
FOINIT	27.3	POROUS	25.5
VDP	-5.8	THICK	25.5
SORW	0.9	WAG	22.5
XKRWE	0.7	VDP	-18.4
XKROE	-.07	XKROE	18.3
VOIL	0.4	FOINIT	15.3
VISC	-0.4	VWAT	14.7
		XKRWE	-14.6
		QRES	13.4
		SORW	12.7
		VISC	-7.5
		VOIL	-6.1
		XKRGE	-3.4
		SALN	-2.0
		DELC3	-1.9

G. Discussion

The results of comparison runs with the carbon dioxide predictive simulator CO2DIP are complete. The CO2DIP simulator has shown reasonable matches with the field results of the Slaughter Estate pilot unit.[10] Sensitivity studies have been made on all input variables, and the results have been shown for the Slaughter Estate pilot unit.

Modifications were made in subroutine PATH to update the slow path algorithm to include an immiscible CO_2 gas phase. Changes were made to perform the equilibrium flash calculations on the same two phase basis as in the miscible model. The presence of a third, immiscible, gas phase affects only the fractional flow calculations, not the thermodynamic equilibration of the oleic and aqueous phases. Under the assumptions of this model, the gas phase does not participate as a true three phase system at equilibrium. This

can be justified assuming that the oil and water are not volatile at low temperatures and moderate pressures.

The algorithm basically converts three phase saturations to obtain equivalent two phase oil and water saturations for use in obtaining equivalent two phase component concentrations. These concentrations are then used to perform the two phase flash calculations. The resultant two phase saturations are then reconverted to three phase values for fractional flow calculations.

The CO_2 immiscible predictive model gives useful results on the Talco field project but cannot be made to work on the Wilmington CO_2 pilot project, which has a production history for matching. The Wilmington pilot has a higher PRES, SWCN, SORW, QRES, and especially a higher VOIL (oil viscosity); however, the real reason appears to be in the relative permeability calculations for Wilmington.

Sensitivity studies have been made on the Talco field immiscible CO_2 project in a similar way to the Slaughter. The range that some of the input variables can assume is more limited with the immiscible model than with the miscible. There appear to remain some unresolved limitations to the CO_2 immiscible predictive model. A dip angle of not much greater than 0.01 for the Lick Creek base case, for example, results in no intersection point being found in the subroutine called CROSS. Another anomaly in the immiscible model is the disparity in the time scale between the 1-D production summary and the 3-D production summary. The variation is by a factor of 5. This may be explained by the fact that the 1-D is calculated independently from the 3-D.

Since most miscible flood projects with very steep dip angles would design the pattern as line drives from injection to production wells, a true history match can never actually be made with the present predictive models. Perhaps a special predictive model, which makes use of well arrangements other than

five-spot, would give a more favorable response for reservoirs with very large dip angles.

H. Results, Conclusions and Recommendations

The LOSFPM compares favorably to the total oil recovery and project life calculated by more complex simulators but intermediate production rates are not comparable. The model does not calculate the light hydrocarbon bank separately and therefore does not predict breakthrough of the light end components. A Peng-Robinson equation of state (EOS) was written but not merged because thermodynamic data on vapor/liquid distribution coefficients or K-values for the individual components of oil are few. When empirical K-value correlations can be determined from actual light oil steamfloods, the EOS procedures should be merged into LOSFPM.

A test run of the CO_2 miscible predictive model with dip showed a reasonable history match to oil production.

The CO_2 immiscible predictive model has application for moderate to low gravity oil systems. The theory incorporated into the predictive model does not adequately handle the light-oil systems as evidenced by the nonconvergence of the solution for the combined fast and slow paths.

NIPER strongly recommends that the CO_2 immiscible predictive model be modularized in a more structured approach for the Fortran coding. The modifications to the code in a structured manner will clarify any existing problems in the model.

REFERENCES

1. Henline, W. D., M. A. Young, and J. T. Nguyen. Topical Report -- Feasibility Study to Modify the DOE Steamflood and CO_2 (MISCIBLE) Flood Predictive Models Respectively to Include Light Oil Steamflooding and Immiscible Gas Drive. NIPER-54, March 7, 1985.

2. Williams, R. L., H. J. Ramey, S. C. Brown, and S. K. Sanyal. An Engineeering Economic Model for Thermal Recovery Methods. SPE paper 8906, 1980.

3. Hsueh, L., K. C. Hong, and J. H. Duerksen. Simulation of High Pressure and High Temperature Steam Distillation of Crude Oils. Pres. at the UNITAR Second Intl. Conf. on Heavy Crude and Tar Sands, Caracas, Feb. 7-17, 1982, paper UNITAR/CF10/VIII/2.

4. Wilson, G. M. A Modified Redlich-Kwong Equation of State, Application to General Physical Data Calculations. Paper presented at the 65th National AIChE Meeing, Cleveland, 1969.

5. Aydelotte, S. R. and G. W. Paul. Development and Verification of Simplified Prediction Models for Enhanced Oil Recovery Application: Steamflood Predictive Model. Department of Energy Report No. DOE/BC/10327-21, October 1984.

6. Aziz, K., and Ramesh, A. B. Fourth SPE Comparitive Solution Project: A Comparison of Steam Injection Simulators. SPE paper 13510, 1985.

7. Paul, G. W. Development and Verification of Simplified Prediction Models for Enhanced Oil Recovery Applications: CO_2 (Miscible Flood) Predictive Model-Final Report. Department of Energy Report No. DOE/BC/10327-20, October 1984.

8. Orr, F. M., Jr. Simulation of the One-Dimensional Convection of Four-Phase, Four-Component Mixtures. Department of Energy Report No. DOE/ET/12082-8, June 1980.

9. Koval, E. J. A Method for Predicting the Performance of Unstable Miscible Displacements, Soc. Pet. Eng. J., June 1963.

10. Adler, J. C. and Stein, M. H. Slaughter Estate Unit Tertiary Miscible Gas Pilot Reservoir Description. J. Pet. Tech., May 1984.

```
      IF (ABS(ROG).GT.0.) GO TO 1901
      GO TO 146
1901  SG(4)  = (1.- SW(4))/(1.+ ROG)
      SO(4)  = 1 - SG(4) - SW(4)
      IF (SO(4) .LT. SOR(4)) SOR(4) = SO(4)
146   CONTINUE
      XAVG   = SG(4) * RHSTM(4) / (SG(4) * RHSTM(4) + SW(4) *
      RHWAT(4))

      CALL FFLOW(4)
      R4     = SQRT((AREA4 + CELA4(IJ1P1)) / PII)
      FPV(4) = (AREA4 + CELA4(IJ1P1)) / ACRES / 43560.
      IF (ABS(STRIAL-SW(4)).LE. 1.0E-3) GO TO 6000
      STRIAL = SW(4)
      IF (ABS(SO(4)).LE.1.0E-4) GO TO 6000
      CALL ZFLAST(NERROR,TDEW,TSZ)
      IF (NERROR .NE. 1) GO TO 2000
      CALL ZBLAST
      ROG    = (TLA*RHGAS(4)*MWO)/(TVA*RHOIL(4)*MWG)
      GO TO 5000
2000  IF (TSZ .GT. TDEW) GO TO 4000
      GO TO 6000
4000  SO(4)  = 0.0
      SOR(4) = SO(4)
      SG(4) - 1. - SW(4)
```

```
      GO TO 6000
5000 SG(4)  = (1.-SW(4))/(1.+ROG)
      SO(4)  = 1.-SW(4)-SG(4)
      IF (SO(4) .LT. SOR(4)) SOR(4)=SO(4)
6000 CONTINUE
```

APPENDIX B. Test for the Bubblepoint Temperature.

```
      SUBROUTINE BUBPT(TBB,PB)
      COMMON /PROPT/ ACF(7),CMW(7),VD(7),ZC(7),PC(7),TCB(7),TR(7),
     1    PR(7),CI(7,7),ICCOM(7),CMGA(7(,TBA(7)
      COMMON /FRACT/ XQ(7),YQ(7),ZQ(7),FV,FL

      DIMENSION TREC(7),FREC(7),YKEC(7),YEC(7)

      TBB  = 1700.0
      DELT = 200.0
  901 DO 10 ITK = 1,7
      TREC(ITK) = TBB /TCB(ITK)
      PREC(ITK) = PB / PC(ITK)
      YKEC(ITK) = EXP(5.37*(OMGA(ITK))*(1.-1./TREC(ITK)))/PREC(ITK)
   10 CONTINUE
      SYEC = 0.0
      DO 20 ITK=1,6
      YEC(ITK) = ZQ(ITK)*YKEC(ITK)/(1.-ZQ(7))
      SYEC = SYEC + YEC(ITK)
   20 CONTINUE
      DIFT  = SYEC - 1.0
      TOSYE = 1.E-5
      IF (ABS(DIFT) .GT. 1.0) GO TO 2000
      IF (ABS(DIFT) .LE. TOSYE) GO TO 1000
      DELT  = 125.0*ABS(DIFT)
      TBB   = TBB - SIGN(1.,DIFT)*DELT
```

```
      IF (ABS(TBB-DELT).LE.100.) GO TO 1000
      GO TO 901
 2000 TBB   = TBB - SIGN(1.,DIFT)*DELT
      IF (ABS(TBB-DELT).LE.100.) GO TO 1000
      GO TO 901
 1000 CONTINUE
      RETURN
      END

      TEST FOR THE DEWPOINT TEMP.
      SUBROUTINE DEWPT(TDP,PMFS)
      COMMON /PROPT/ ACF(7),CMW(7),VC(7),ZC(7),PC(7),TCB(7),TR(7),
     1    PR(7),CI(7,7),ICCOM(7),CMGA(7),TBA(7)
      COMMON /FRACT/ XQ(7),YQ(7),ZQ(7),FV,FL

      DIMENSION TREC(7),PREC(7),XKEC(7),XEC(7)

      TDP  = 1700.0
      DELT = 70.0
  901 PD   = PMFS

      DO 10 ITK = 1,7
      TREC(ITK) = TDP / TCB(ITK)
      PREC(ITK) = PD / PC(ITK)
      XKEC(ITK) = EXP(5.37*(OMGA(ITK))*(1.-1./TREC(ITK)))/PREC(ITK)
   10 CONTINUE
      SXEC = 0.0
```

```
      DO 20 ITK-1,6
      XEC(ITK) = ZQ(ITK)/XKEC(ITK)
      SXEC = SXEC + XEC(ITK)
   20 CONTINUE
      DIFT = (SXEC - 1.0)
      TOSXE = 1.E-5
      IF (ABS(DIFT) .LE. TOSXE) GO TO 1000
      IF (ABS(DIFT) .LT. 1.0) DELT = 70.0*ABS(DIFT)
      TDP  = TDP + SIGN(1.,DIFT)*DELT
      IF (ABS(TDP-DELT).LE.100.) GO TO 1000
      GO TO 901
 1000 CONTINUE
      RETURN
      END

      SUBROUTINE MOFRACS(TU,PU)
      COMMON /PROPT/ ACF(7),CMW(7),VC(7),ZC(7),PC(7),TCB(7),TR(7),
     8    PR(7),CI(7,7),ICCOM(7),CMGA(7),TBA(7)
      COMMON /FRACT/ ZQ(7),YQ(7),ZQ(7),FV,FL
      COMMON /MOFRA/ TVA,TLA

      DIMENSION KET(7),TREC(7),PREC(7),VA(7),LA(7)
      REAL L,LA,KET

      DO 300 ITK = 1,7
      TREC(ITK)  = TU /TCE(ITK)
      PREC(ITK)  = PU / PC(ITK)
```

```
      KET(ITK)    = EXP(5.37*(OMGA(ITK))*(1.-1./TREC(ITK)))/PREC(ITK)
  300 CONTINUE
      DELTA = 0.1
      L = 0.2
      V = 0.8
  445 L = 1. - V
      TVA = 0.0
      DO 400 ITK-1,6
      VA(ITK) = ZQ(ITK) / (1.+ (1./ KET(ITK))*(L/V))
      TVA = TVA + VA(ITK)
  400 CONTINUE
      VA(7) = ZQ(7)
      TVA = TVA+VA(7)
      TLA = 0.0
      DO 500 ITK = 1,6
      LA(ITK) = ZQ(ITK) - VA(ITK)
      TLA = TLA + LA(ITK)
  500 CONTINUE
      LA(7) = 0.
      DIFA  = TVA - V
      TOLA  = 1.E-5
      IF (ABS(DIFA) .LE. TOLA) GO TO 1500
      DELTA = 0.1 * ABS(DIFA)
      V = V + SIGN(1.,DIFA)* DELTA
      GO TO 445
 1500 TXQ   = 0.0
      DO 600 ITK = 1,6
```

```
      XQ(ITK) = LA(ITK)/TLA
      TXQ   = TXQ + XQ(ITK)
600 CONTINUE
      XQ(7) = 0.
      TYQ   = 0.0
      DO 602 ITK = 1,7
      YQ(ITK) = VA(ITK)/TVA
      TYQ   = TYQ + YQ(ITK)
602 CONTINUE
      RETURN
      END

      SUBROUTINE ZFLAST(NERROR,TCPT,TSZ)
      REAL MWCP,MWGP,MWOK,MWATC,MWO,MWGK,MWGS,MWG
      CHARACTER* 16 COMP
      COMMON /CHARA/ COMF(15)
      COMMON /COUNT/ NCOMP,ITMAXB

      COMMON /PROPT/ ACF(7),CMW(7),VC(7),ZC(7),PC(7),TCB(7),TR(7),
     1    PR(7),CI(7,7),IDCCM(7),OMGA(7),TBA(7)

      COMMON /FPRCP/
     * API, RS, VIS80, VIS100, VIS210, VIS1, VIS2, SGO, SGW, SG
     1 KRO(4),   KRW(4),    KRG(4),    PGD(4),
     2 VISO(5),  VISW(5),   VISG(5),   VISS(5),   BMW(7),
     3 FOIL(4),  FWAT(4),   FGAS(4),
     4 RHOIL(4), RHWAT(4),  RHGAS(4),  RHSTM(4), DENB(7),
```

```
     5 SOR(4),    SWR(4),    SGR(4),
     6 SG(4),     SO(4),     SW(4),     PV(4),     ROS,
     7 BTA(3),    PRS(4),    TMP(4),    FPV(4),
     8 BO(4),     BW(4),     BG(4),     MOBIL(4)
       REAL
     9 KRO, KRW, KRG, MOBIL

       COMMON /FRACT/ XQ(7),YQ(7),ZQ(7),FV,FL
       COMMON /TRIAL/ VL
       COMMON /MOFRAC/ TVA,TLA
       COMMON /MOLEC/ MWO,MWG

       DIMENSION DENL(7), MWOP(7),MWGP(7)
       DENW = 62.4
       WMW  = 18.01
       DENK = 0.0
       DO 10 IB = 1,6
       DENL(IB) = (XQ(IB)*DENB(IB))
       DENK     = DENK + DENL(IB)
    10 CONTINUE
       WATC = XQ(7)*DENW
       DENO = DENK + WATC
       MWOK = 0.0
       DO 20 IB = 1,6
       MWOP(IB) = XQ(IB)*EMW(IB)
       MWOK     = MWOK + MWOP(IB)
    20 CONTINUE
```

```
      MWATC = XQ(7)*WMW
      MWO   = MWOK + MWATC
      XB    = (SC(4)*DENO)/MWO
      MWGK  = 0.0
      DO 30 IB = 1,6
      MWGP(IB) = YQ(IB)*BMW(IB)
      MWGK     = MWGK + MWGP(IB)
   30 CONTINUE
C     TEMPERATURE (TMF) IS IN R DEGREE.
      TMF = TMP(4) + 459.69
      PMF = PRS(4)
      CALL DEWPT(TDPT,PMF)
      CALL BUBPT(TBP,PMF)
      IF (TMF .LT. TBP .OR. TMF .GT. TDPT) GO TO 3000
      NERROR = 1
      CALL MOFRACS(TMF,PMF)
      GO TO 1650
 3000 NERROR = 0
 1650 TSZ = TMF
      RETURN
      END
```

APPENDIX C. Bisection Algorithm.

Bisection Algorithm for Calculating Phase Saturations Injected:

```
      S30   = 0.0001 + S3R
      S31   = .9999-S1R-S2R
      SR    = 1.-S1R-2SR-S3R
      TOLI  = 1.E-6
      ITI   = 0
      FUNCO = WAG -(V(3)/V(1))*(KR1E/KR3E)
     1 *((1.-S2R-S30-S1R)/SR)**M
     2 /((S30-S3R)/SR)**MN
   29 ERROR = ABS(S31-S30)
      ERROR = ERROR/2.
      IF (ERROR .LE. TOLI) GO TO 31
      XM    = (S31+S30)/2.
      FUNCM = WAG -(V(3)/V(1))*(KR1E/KR3E)
     1 *((1.-S2R-XM-S1R)/SR)**M
     2 /((XM-S3R)/SR)**MN
      IF(FUNCO*FUNCM .LE.0.) GO TO 30
      S30   = XM
      FUNCO = FUNCM
      GO TO 29
   30 S31   = XM
      GO TO 29
   31 CONTINUE
      S3    = S31
      S2    = S2R
```

```
S1    = 1.-S2-S3
S1PI  = S1
S2PI  = S2
S3PI  = S3
```

APPENDIX D. Modification to Subroutine FRACT.

```
C COMPUTE FRACTIONAL FLOW ALONG FAST PATH (FROM INITIAL)
C
  IPTH  = 1
  S(3)  = 0.0
  CALL PATH
C
C COMPUTE FRACTIONAL FLOW ALONG SLOW PATH (FROM INJECTED)
C
  IPTH  = -1
  S(3)  = S31
  CALL PATH
```